Available online at www.sciencedirect.com
ScienceDirect
Journal of Sound and Vibration 299 (2007) 419–459
JOURNAL OF SOUND AND VIBRATION
www.elsevier.com/locate/jsvi

Review

Aeroacoustics research in Europe: The CEAS-ASC Report on 2005 highlights

Spyros G. Voutsinas*

National Technical University of Athens, School of Mechanical Engineering, 9 Heroon Polytechniou Str, 15773 Athens, Greece

Received 13 March 2006; received in revised form 10 April 2006; accepted 11 April 2006

Abstract

This paper summarizes some of the aeroacoustic research undertaken in Europe in 2005. It is compiled from information provided by the Aearocoustics Specialists' Committee (ASC) of the Confederation of European Aerospace Societies (CEAS). The committee comprises representation from the Aerospace Societies of France (AAAF), Germany (DGLR), Italy (AIDAA) the Netherlands (NVvL), Spain (AIAE), Sweden (SVFW) and the United Kingdom (RaeS) together with members from Greece, Ireland, Poland and Portugal.

Contents

*Tel.: +30 2107721096; fax: +30 2107721057.
E-mail address: spyros@fluid.mech.ntua.gr.

0022-460X/$ - see front matter © 2006 Elsevier Ltd. All rights reserved.
doi:10.1016/j.jsv.2006.04.032

1. Introduction

The role of the Aeroacoustics Specialists' Committee (ASC) of the Confederation of European Aerospace Societies (CEAS) is to promote and encourage activities on aeroacoustics in the industrial and research communities in Europe. This paper gives a concise overview of some of the most important activities conducted during 2005. Reports have been collected through the national representatives, members of ASC and are presented in a thematic breakdown. An exception has been made for Significantly lower community exposure to aircraft noise (SILENCE(R)) which is presented first, due to its significance to aeroacoustics research. Finally enquiries concerning all contributions should be addressed to the authors who are given at the end of each subsection.

2. Significantly lower community exposure to aircraft noise

SILENCE(R) is the largest project on aircraft noise ever supported by the European Commission. As part of the Framework 5 "Growth" programme, it started on 1 April 2001, and its end date is 30 June 2006.

SILENCE(R) has a budget of 111 million euros, about 50% of which is funded by the EC, and is carried out by 51 partners: the large European aerospace industries, research establishments, SME's, and universities. The coordinator of this consortium is Snecma.

The project is focused on the development of aircraft noise reduction technologies. Its main objectives are:

- Validation of individual technologies
- Identification of applicability over the product range
- Cost/benefit analysis

The research and development activities are carried out in the fields of nacelle technology, engine source noise, and airframe noise. More than 35 prototypes have been put to test during the SILENCE(R) programme. Now that SILENCE(R) has entered its last phase, the most promising technologies that were developed during the first phase, are now tested in large-scale rigs or by means of flight tests.

This contribution describes some recent highlights.

2.1. Nacelle technology

Research is carried out on both the nacelle design itself and on the acoustic liners. One of the possibilities for a low-noise nacelle is the application of a so-called negatively scarfed intake (NSI), see Fig. 1.

The idea behind this design is to change the directivity pattern of the noise radiation, so that more noise will be radiated upward, and less noise downward. After extensive wind tunnel testing on scale models, flight tests with an NSI mounted on one of the engines of an Airbus A320 have been carried out in Moron (Spain) and Tarbes (France). Data analysis is still under way. Part of the research on nacelle acoustic liners was focused on the development and assessment of zero-splice inlet liners, see Fig. 2.

As conventional liners are manufactured in several pieces (typically 3), splices are formed where the pieces are joined. It is well known that these splices have a negative effect on the performance of the liners, not only because of the reduced area covered by lining material, but also because the splices cause the prevailing circumferential acoustic modes to scatter to other modes, which are less effectively attenuated. Large-scale research on zero-splice inlet liners has been carried out in the Anecom Aerotest facility, see Fig. 3. This is the first SILENCE(R) technology that has been taken into production (on the Airbus A380). As can be seen in Fig. 4, a significant improvement was found by application of the zero-splice liner.

Fig. 1. Negatively scarfed intake.

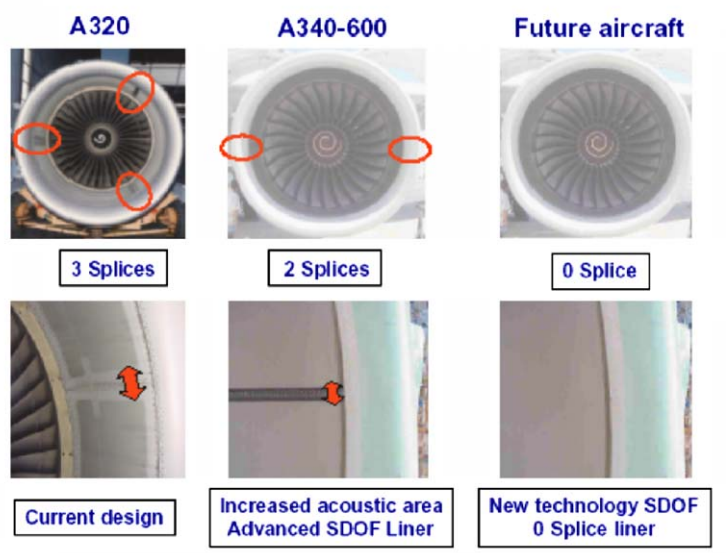

Fig. 2. Splices in inlet liners.

2.2. Engine source noise

The research on engine noise in SILENCE(R) encompasses all relevant sources: fans, compressors, turbines, and jets. Low noise fan designs were tested at large scale in the Anecom Aerotest facility.

To reduce jet noise, alternative shapes of the exhaust nozzle are investigated. In Fig. 5, an example is shown of a 'squid' nozzle, tested in a wind tunnel. The serrations at the nozzle have an effect on the vortex shedding, thereby reducing the mixing noise generated in the jet. A similar nozzle as shown in Fig. 5 was eventually tested in flight.

2.3. Airframe noise

Although the noise from both high lift devices and landing gears was investigated, the emphasis of the large-scale tests was put on the latter. Flight tests have been carried out on landing gears equipped with aerodynamic fairings, as shown in Fig. 6.

Extensive measurements have been carried out, with microphones mounted on the aircraft, and phased microphone arrays on the ground. Due to the fairings, a noise reduction of about 1.8 EPNdB has been achieved [E. Kors, SNECMA, eugene.kors@snecma.fr and H. Brouwer, NLR, brouwer@nlr.nl].

3. Fan and jet noise

3.1. TURNEX

In January 2005 was the official start of the 6th Framework EU-project TURNEX (Turbomachinery Noise Radiation through the Engine Exhaust). A consortium of 12 partners, coordinated by the Institute of Sound and Vibration Research (ISVR), is working on the understanding and reducing of the radiation of turbomachinery noise from exhaust nozzles.

3.1.1. Background

Research is needed to develop innovative concepts and enabling technologies to reduce aeroengine noise at source. Turbomachinery noise radiating from the bypass and core nozzles is becoming the dominant noise

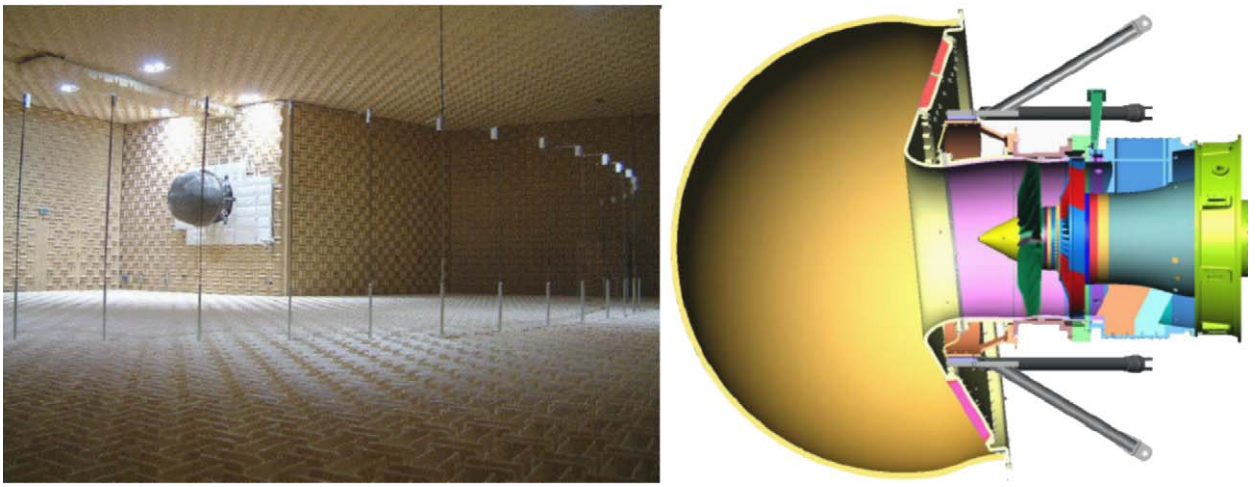

Fig. 3. Anecom Aerotest facility and engine model with Turbulence Control Screen.

source on modern aircraft, but, while recent EU research programmes have made significant progress in reducing both the generation of turbomachinery noise and the radiation of noise from the intake, little work has been conducted on reducing the radiation of turbomachinery noise from exhaust nozzles. TURNEX will address this shortfall by delivering improved understanding and validated design methods, and by evaluating a number of low-noise exhaust nozzle configurations aimed at a source noise reduction of 2–3 dB.

Description of the work and objectives (Fig. 7).

WP 1: Turbomachinery noise radiation experiments on an engine exhaust rig in a Jet Noise Test Facility. The main objective is to experimentally test at model scale (a) innovative noise reduction concepts, including a scarfed exhaust nozzle, and (b) conventional engine exhaust configurations. The experiments will develop and utilise simulated turbomachinery noise sources and innovative measurement techniques in order to realistically evaluate the noise reduction concepts and to provide a high-quality validation database. A secondary objective is to technically assess the relative merits of different methods of estimating far-field noise levels from in-duct and near-field noise measurements, using both models and the validation data, to enhance the capability of European fan noise test facilities to simulate fan noise radiation through the exhaust.

WP 2: Improved Models and Prediction Methods. The objective is to improve models and prediction methods for turbomachinery noise radiation through the engine exhaust, to a level comparable with that being achieved for intake radiation, and validate those with the experimental data.

WP 3: Assessment and Industrial Implementation of Results. The objective is to conduct a parametric study of real geometry/flow effects (pylons, flow-asymmetry) and noise reduction concepts (scarfed nozzles, acoustically lined after-body) as applied to current and future aircraft configurations of interest.

3.1.2. Expected results

TURNEX will deliver validated industry-exploitable methods for predicting turbomachinery noise radiation through exhaust nozzles, allowing EU industry to leapfrog NASA-funded technology developments in the US. It will also deliver a technical assessment on the way forward for European fan noise testing facilities and an assessment of exhaust nozzle concepts for noise reduction at source [by B.J. Tester, ISVR, United Kingdom].

3.2. "Buzz-saw" noise: a comparison of measurement with prediction

"Buzz-saw" noise is radiated from a turbofan inlet duct when the fan tip speed is supersonic. Accurate prediction of this noise source necessitates consideration of nonlinear acoustics, modelling a complete fan blade set, modelling an acoustic liner, and calculations at high frequencies. A series of papers have described work concerning the application of one-dimensional propagation models to the prediction of buzz-saw noise

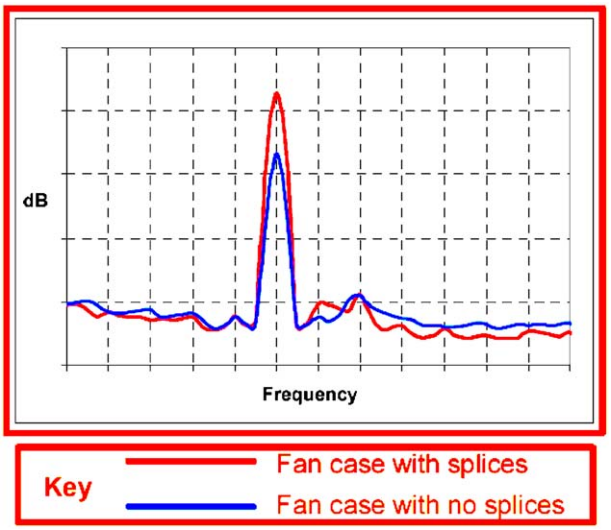

Fig. 4. Acoustic spectrum showing the effect of splices.

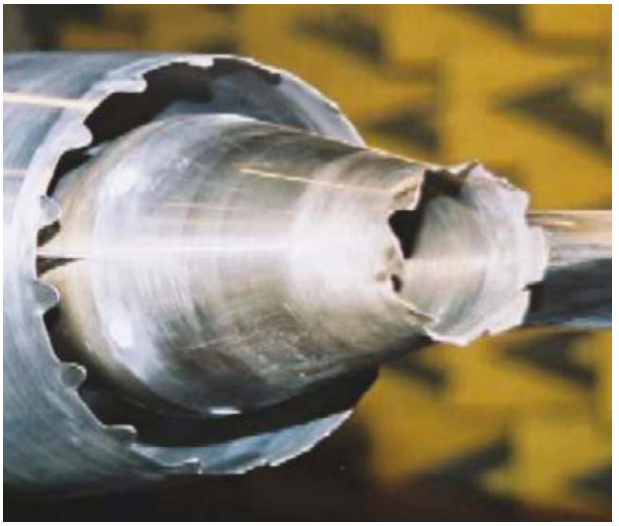

Fig. 5. Model of a 'squid' nozzle.

[1,2]. A numerical model, termed the Frequency Domain Numerical Solution or FDNS, is used to calculate the nonlinear propagation of the rotor-alone pressure field in an acoustically lined inlet duct. From this the in-duct noise level of the buzz-saw tones can be determined. More recently, new measurements of buzz-saw noise in a lined inlet duct have been utilized. A detailed set of validation test cases are presented in [3]. These show comparison of measurement with prediction. Also, the measurements reveal the effect of an acoustic liner on buzz-saw noise. A typical example is shown in Fig. 8. Also, various different aspects of the noise problem have been examined. These include the effect of the inlet duct wall boundary layer on attenuation of sound, and a modal breakdown which identifies the levels of the rotor-alone and non-rotor-alone buzz-saw noise sources [by A. McAlpine, ISVR, University of Southampton, UK am@isvr.soton.ac.uk].

3.3. Noise radiation from bypass ducts

An analytical model was developed for sound radiation from turbofan bypass ducts [4]. This problem is modelled by a semi-infinite un-flanged annular duct carrying a jet that issues into a uniform mean flow.

Fig. 6. Airbus A340 main landing gear equipped with fairings.

The turbofan after-body is represented by an infinite cylindrical centre body extending downstream from the duct exit. Noise propagates along the annular bypass duct, refracts through the external bypass stream and radiates to the far field. The instability wave of the vortex sheet and the refraction of sound waves by the jet shear layer are accounted for in an exact way. Good agreement was found between analytical solutions and experimental data from the ANCF test rig at NASA Glenn Research Center [5], see Fig. 9. The capability to obtain near field solutions is particularly useful in providing reference solutions with which to assess extensively the accuracy of numerical solutions, see Fig. 9. The problem of sound radiation from a jet pipe includes most of the difficulties that need to be addressed in general applications of computational aeroacoustics to aero-engines, such as the scattering by duct terminations, radiation to the free field, wave refraction at vortex layers and the presence of instability waves. An interesting feature of the analytical solution is that it is possible to separate explicitly the instability wave from the rest of the solution [by G. Gabard, R.J. Astley, ISVR, University of Southampton, UK, gg1@isvr.soton.ac.uk, rja@isvr.soton.ac.uk].

3.4. Numerical simulation of fan tone noise

In the framework of general studies relative to fan tone noise prediction, a computation procedure has been recently developed at ONERA in order to provide a full numerical simulation, including source generation, acoustic propagation in the duct, and radiation by inlet or outlet. Noise sources are given by a 3D RANS (Reynolds Averaged Navier–Stokes) computation, using ONERA CFD platform *elsA*. CFD outputs are post-processed using a modal expansion of pressure disturbances over acoustic cut-on modes. These modes then are expressed in terms of equivalent sources (using a monopole distribution) in a 3D-structured a sixth-order Euler solver, *sAbrinA*, also developed at ONERA [6]. *sAbrinA* simulates in-duct propagation and near-field

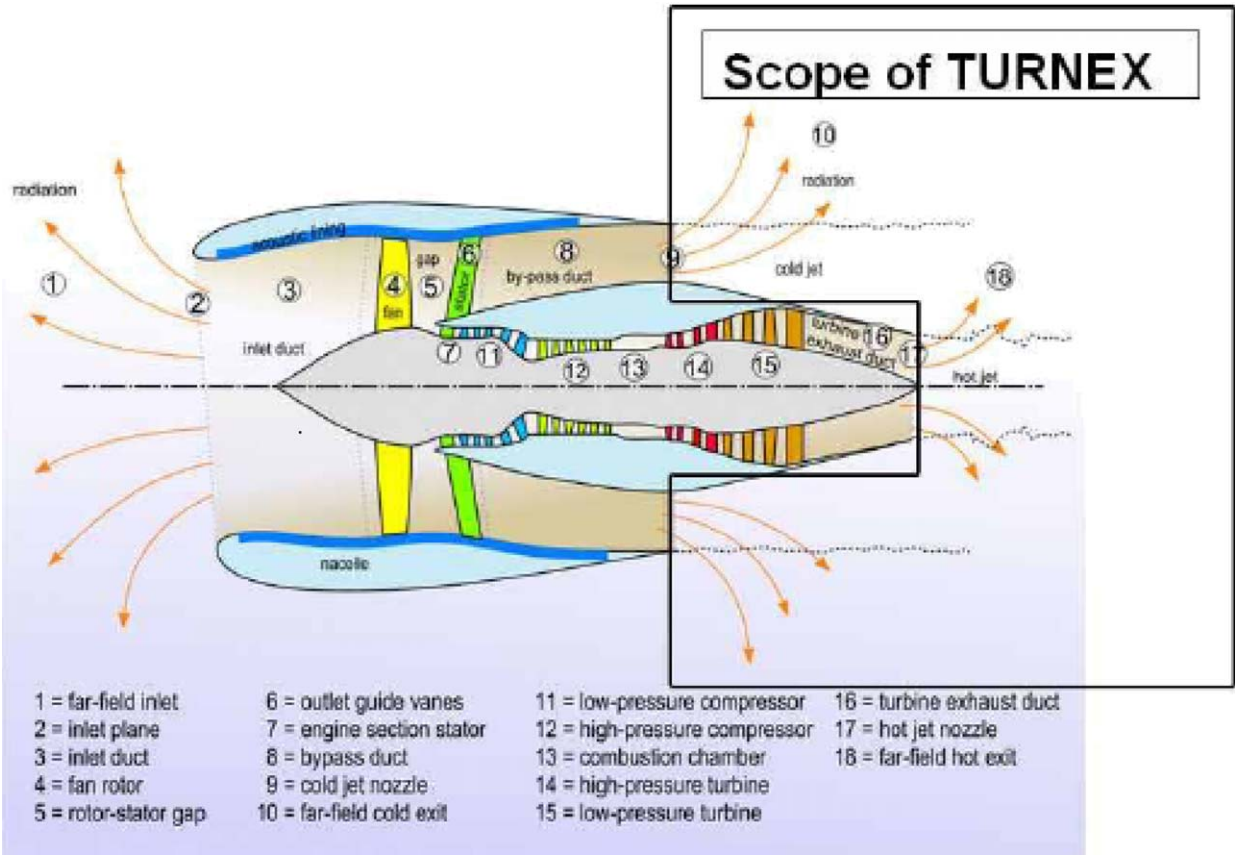

Fig. 7. Scope of TURNEX.

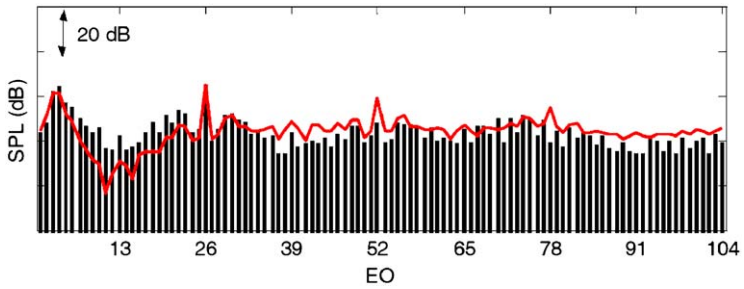

Fig. 8. Measured EO frequency spectrum in an acoustically-lined inlet duct. Relative Mach number of flow impinging on fan blades, $M_{rel} = 1.28$. The fan has 26 rotor blades, i.e. blade passing frequency is EO = 26. The numerical prediction is shown by the solid red line.

radiation in the vicinity of the inlet (or the outlet). Far-field radiation is extrapolated by the use of a Kirchhoff integral, written in the frequency domain.

First validations of computation chain *elsA–sAbrinA* [7] have been applied to a turbofan model tested in the DNW-LLF anechoic wind tunnel, in the framework of European DUCAT project, and also used as a reference case in the TurboNoiseCFD project. Fig. 10 shows a simulation with *elsA* of the generation of angular mode of order $m = -2$, due to the interaction between the rotor wake (16 blades) and the stator (18 vanes). A simulation with *sAbrinA* of acoustic propagation and radiation of this mode is shown in Fig. 11. Far-field directivities upstream of the inlet obtained by coupling *sAbrinA* with the Kirchhoff method are in a very good agreement with experiment, as shown in Fig. 12. In particular, clearance patterns due to

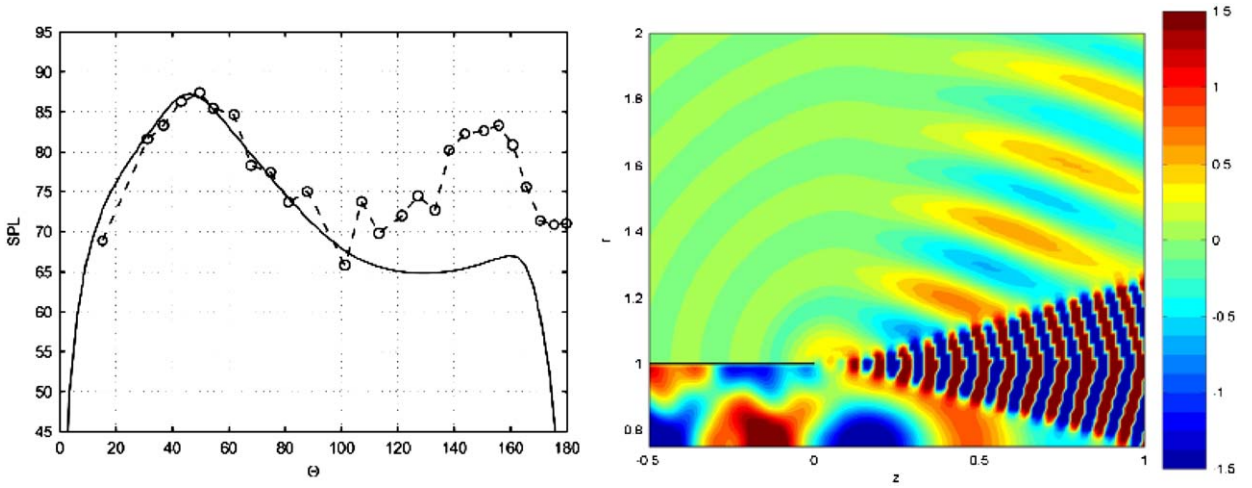

Fig. 9. Left: comparison of analytical solution (solid line) with experimental data (dashed line) for the far-field directivity with an incident mode (2,0) at 533 Hz with a 0.175 jet Mach number. Right: example of near-field pressure for the mode (17,1) at 1623 Hz with a 0.45 jet Mach number (note the presence of the instability wave).

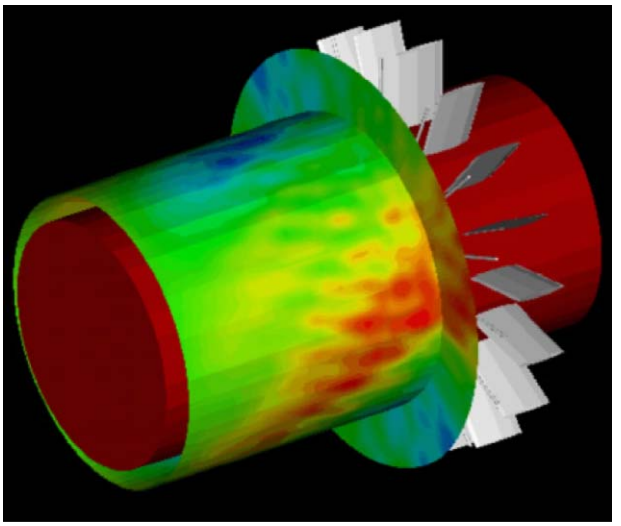

Fig. 10. Rotor–stator interaction using 3D RANS computations (*elsA*).

interferences between upstream (from inlet) and aft (from outlet) radiation, both included in the computations, are perfectly assessed.

As a next step, the computation procedure is going to be used to provide an aeroacoustic analysis of a SNECMA counter-rotating turbofan, designed in the framework of the VITAL Integrated Project [by C. Polacsek, ONERA, France].

3.5. Sound production by coherent structures in subsonic jets

Pressure measurements performed in the irrotational near-field of a Mach 0.3 jet with a Reynolds number of 300,000 revealed an interference mechanism between the reactive and propagative components of the pressure field, characterised respectively by axial convection (at 70% of the jet exit velocity) and spherical, sonic propagation. A simple model was successfully used to capture the essential features of the interaction mechanism. The assumptions involved in the model imply quasi-irrotational sound production at the heart of

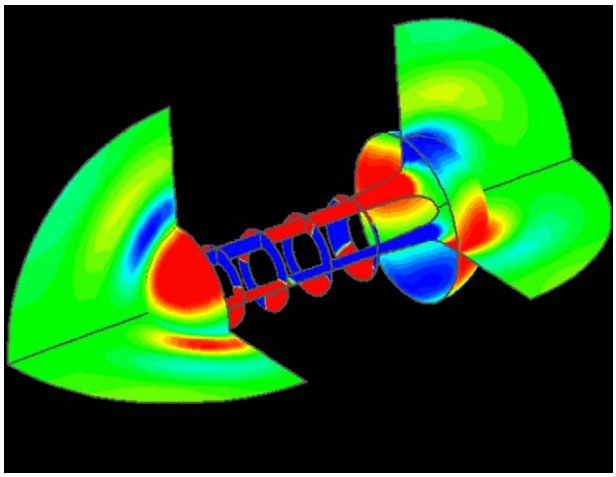

Fig. 11. Acoustic propagation of interaction mode using 3D Euler computations (*sAbrinA*).

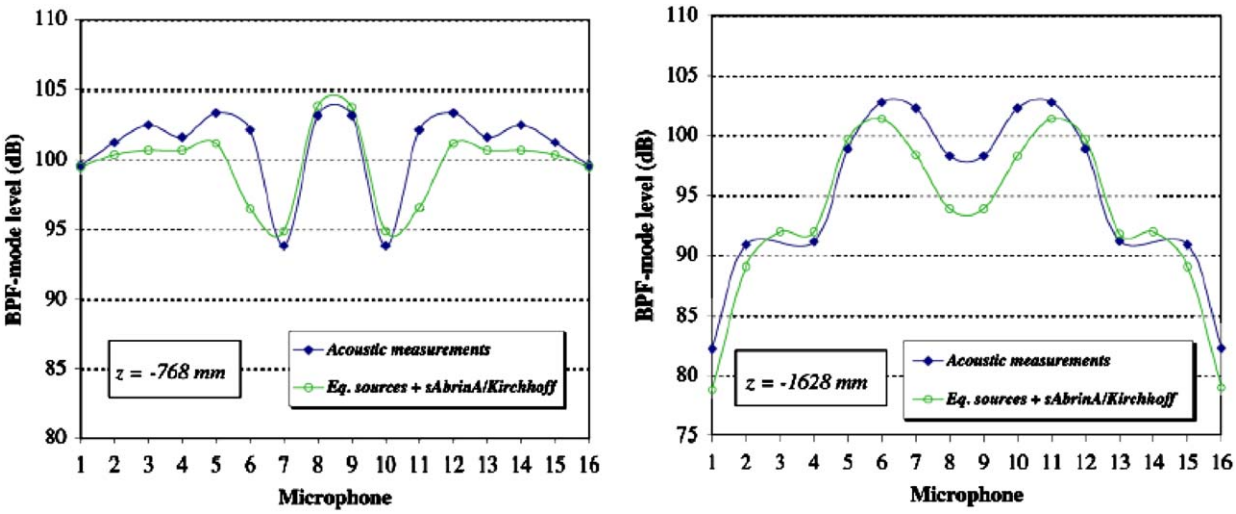

Fig. 12. Comparison between numerical and experimental directivities upstream of DUCAT turbofan model.

the rotational mixing-layer, indicating that coherent structures in the initial regions of the jet produce sound by a wavy-wall type mechanism [8]. Further experiments using an azimuthal near-field microphone array were used to demonstrate how higher order azimuthal modes (modes 0–4) also participate in this interference mechanism, showing that these too produce sound in this quasi-irrotational fashion [9]. The implication of this work is that at least some part of the sound production mechanism of the subsonic jet can be modelled using an instability-wave approach [by P. Jordan, Université de Poitiers, France].

3.6. Prediction of turbofan rotor or stator broadband noise radiation

Fan broadband noise has become the major component of overall sound levels radiated by modern turbofans due to past progress in tone reduction. It is expected that forward radiation is mainly due to the rotor, but that aft radiation comes from the outlet guide vanes. It is the reason why present studies now extend earlier calculations on rotor acoustics towards a unified model predicting either rotor or stator upstream and downstream radiation.

In the present model, sources are limited to blade and vane random loads which are known to be the main terms. A generic flat spectrum decreasing at high frequency is used as input, in accordance with several tests. The analytical Green's function in a hard-walled cylindrical duct is implemented in the Ffowcs-Williams and Hawkings equation to compute sound propagation in the nacelle. Directivity of free-field radiation is deduced using either a Rayleigh integral (Tyler and Sofrin model) or a Kirchhoff integral on the duct exit cross-section.

Forward radiated sound power spectra and directivities are in good agreement with test data and existing semi-empirical predictions such as that of Heidmann at NASA (Fig. 13a). There are on the contrary large discrepancies on directivities downwards (Fig. 13b), due to refraction in the hot jet at a higher speed [10]. It means that aft radiation will require computation of linearized Euler equations (LEE) in the actual flow field.

Overall sound power levels, OAPWL, emitted upstream (label "Up") and downstream (label "Down") by the rotor and the stator are plotted in Fig. 14 as a function of the rotation speed (with a logarithmic scale). OAPWL are computed in two ways, either inside the duct (solid lines) or in the free field (symbols), giving identical results. It has been checked that free-field sound powers computed using the Rayleigh integral give

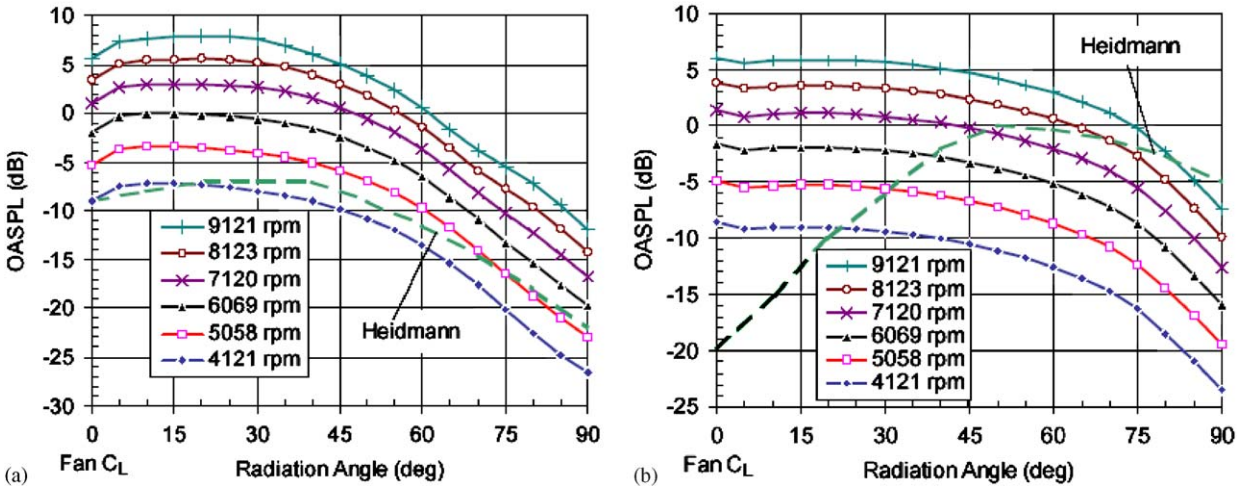

Fig. 13. Free-field directivities of overall sound pressure level, OASPL, at several rotation speeds (Kirchhoff integral). Arbitrary reference of decibels: (a) Upstream radiation from the rotor, (b) Downstream radiation from the stator.

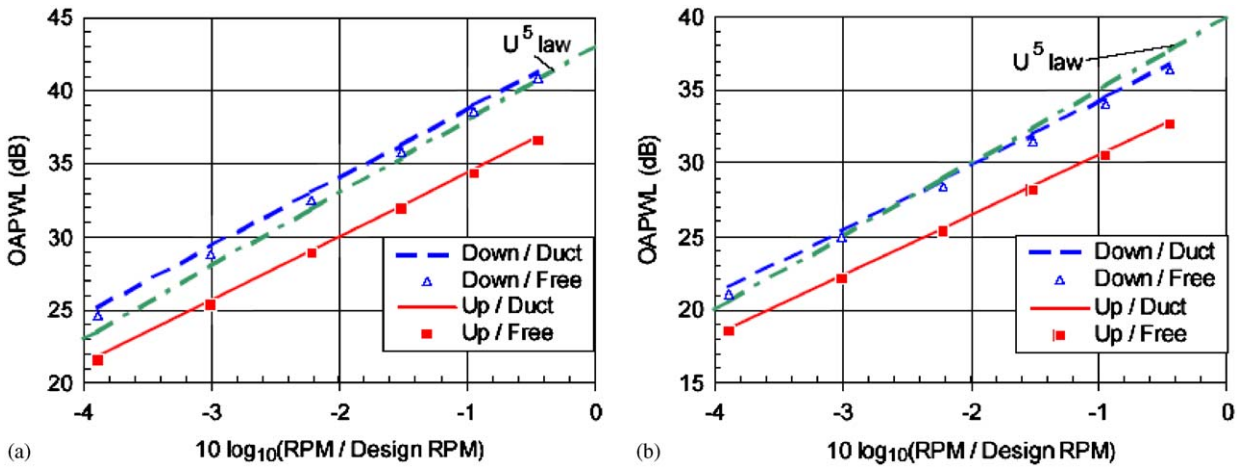

Fig. 14. Overall sound power level, OAPWL, versus rotation speed (in logarithmic scale). Free field computation using Kirchhoff integral. Same reference of decibels as in Fig. 13: (a) Rotor radiation and (b) Stator radiation.

values very close to the Kirchhoff integral, without mean flow. It is also shown that sound powers vary like the velocity to the fifth power which is a conventional law for random dipoles. The radiation is about 3 dB higher downstream than upstream, and the stator noise is 3 dB lower than that of the rotor for the selected input data. These first results, neglecting flow velocity inside the nacelle, suggest that forward radiation from the rotor and aft radiation from the stator would have similar levels.

Next issue will be to introduce more realistic random loads on blades or vanes. Such data will be available from LES computations during the European project PROBAND [by S. Lewy, ONERA, France, Serge.Lewy@onera.fr].

3.7. Prediction of the propagation and radiation of aft-fan and core noise

In approach and cut-back conditions, turbomachinery noise radiating from the bypass and core nozzles is becoming the dominant noise source. To guide the development of innovative solutions in view of reducing the radiation noise from the aft fan duct and core nozzle of modern high bypass ratio turbofan, in which sound propagates through the shear layers of high speed jets, accurate predictions of exhaust noise and aft fan noise are required. This problem represents a challenging task for CAA, due to the presence of the shear layers separating the core, bypass and free-stream fields. While the future probable solution of this problem lies in the development of appropriate numerical models, based on the LEE which can deal accurately not only with the shear layers but also with non-uniform mean flows, simplified models based on the convected wave equation, are useful both for parametric studies and as benchmark solutions for the next generation of numerical models.

In collaboration with AVIO Group, a finite element numerical technique, developed for the solution of the convected wave equation [11], has been applied to the prediction of the propagation and radiation of aft fan noise and core noise including the effect of forward flight. The vortex layers, separating the nozzle core, bypass, and mean-stream flows, are treated as interior boundaries with appropriate boundary conditions. Each sub-domain is subdivided into non-overlapping triangular and quadrilateral elements. Along artificial boundaries, to avoid incoming spurious reflections, appropriate non-reflecting boundary conditions are imposed. On each source boundary, inside the fan and nozzle ducts, an incoming wave is specified. The duct walls are considered as rigid and across the vortex layer interfaces, continuity of the pressure and of vertical displacement are imposed. In addition, the singularity of the solution at the duct lips is avoided by imposing an appropriate Kutta condition [by R. Arina, Politechnico di Torino, Italy, renzo.arina@polito.it].

4. Duct acoustics

4.1. Modal scattering at an impedance transition in a lined flow duct

A Wiener–Hopf solution is derived to describe the scattering of duct modes at a hard-soft wall impedance transition in a circular duct with uniform mean flow, directed from the hard to the soft section [12]. In the absence of experimental evidence, it is particularly interesting to investigate the role of possible vortex shedding from the hard-walled section trailing edge in combination with the edge singularity (Kutta condition or otherwise). In general, the effect of the Kutta condition is significant, but it is particularly large for the plane wave at low frequencies and should therefore be easily measurable. For $\omega \to 0$, the modulus of the reflection coefficient tends to $(1+M)/(1-M)$ without and to 1 with Kutta condition, while the end correction tends to 1 without and to a finite value with Kutta condition (Fig. 15) [by S.W. Rienstra, Eindhoven University of Technology, The Netherlands, N. Peake, Cambridge University, UK].

4.2. Analytic Green's function for a lined circular duct containing uniform mean flow

A complete and explicit analytic expression is derived of the Green's function for a lined circular duct, both hollow and annular, containing uniform mean flow, from first principles by Fourier transformation [13]. In practical applications a closed form analytic Green's function will be computationally more efficient, especially at high frequencies of practical interest to aero-engine applications (Fig. 16) [by S.W. Rienstra, Eindhoven University of Technology, The Netherlands, and B.J. Tester, ISVR, United Kingdom].

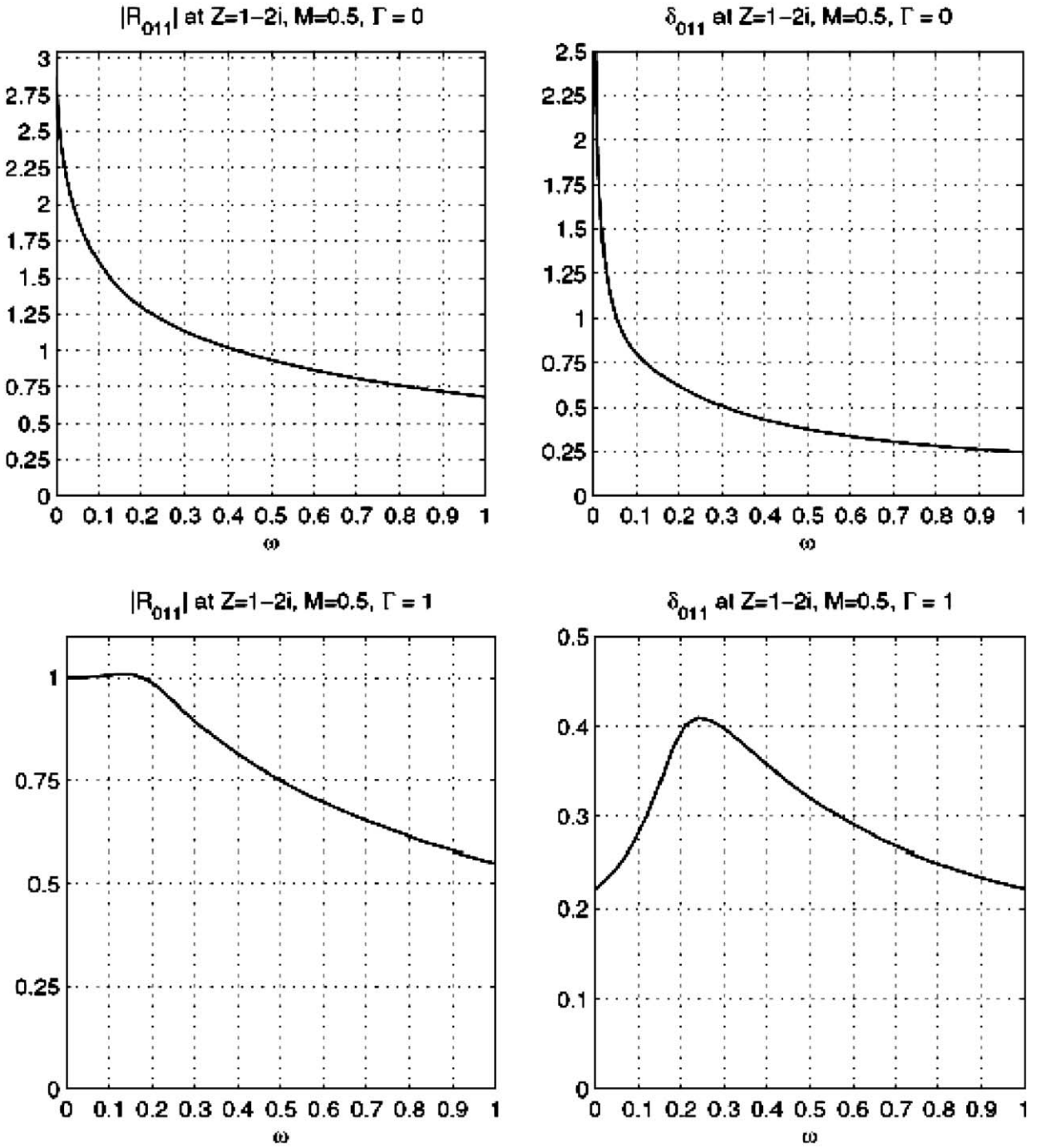

Fig. 15. Modulus of plane wave reflection coefficient and end correction at impedance $Z = 1 - 2i$ and $M = 0.5$, without (upper) and with (lower) Kutta condition.

4.3. Acoustic modes in a ducted shear flow

A robust numerical algorithm for determination of duct eigenmodes in sheared and/or swirling mean flows, in both hard and soft-walled ducts, was developed and tested against available data [14]. The method was shown to be capable of handling very high frequencies (Helmholtz numbers at least as high as 100). An

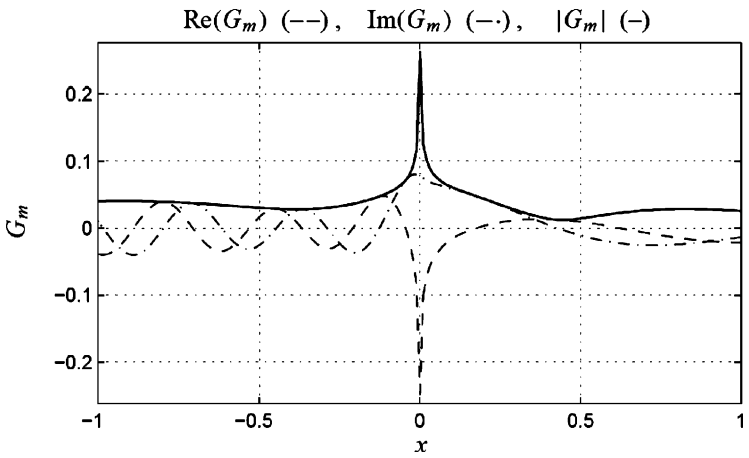

Fig. 16. 3D circumferential Fourier component of Greens function with 400 radial modes at $r = 0.7$, $M = 0.5$, $\omega = 10$, $h = 0.3$, $Z_1 = 1 - i, Z_h = 1 + i$.

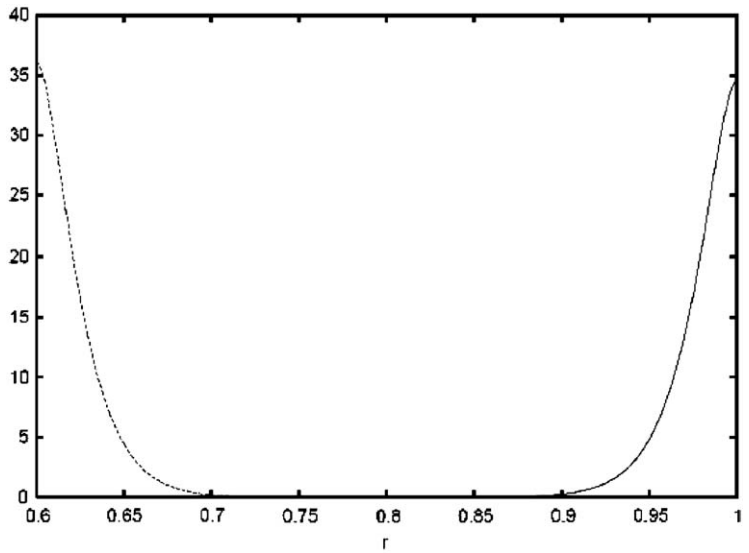

Fig. 17. Hydrodynamic pressure modes (slipping mean flow).

analytical theory for high frequencies, modal wavenumbers and circumferential orders was developed in order to check the proposed algorithm where the independent data was not available and to give insight into the qualitative behaviour of the solutions. The obtained results confirm that for the mean flow profiles with non-zero wall Mach numbers the acoustic eigenmodes are supplemented by a finite number (per circumferential order) of hydrodynamic modes, which are (physically) concentrated near the duct walls (see Fig. 17). For the boundary-layer mean-flow profiles that vanish at the wall a continuous hydrodynamic spectrum is recovered [by G.G. Vilenski and S.W. Rienstra, Eindhoven University of Technology, The Netherlands].

4.4. Acoustic liner modelling

In line with progress experienced in engine source noise reduction, jet noise and airframe noise reductions, it is essential that the nacelle duct acoustic panels are designed to present impedance to the propagated noise which is as closely matched as possible to the optimum impedance desired for maximum attenuation, for each of the flight certification points. Aermacchi have initiated a study to address the measurement and modelling

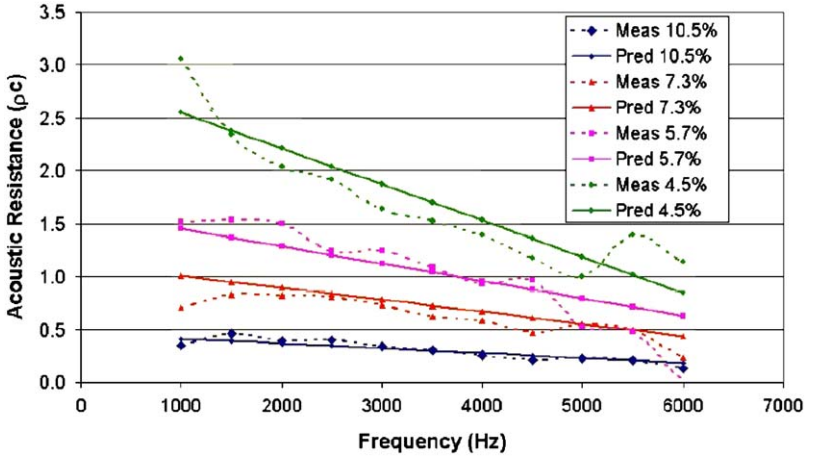

Fig. 18. Liner resistance fit to measurements ($M = 0.3$, cell depth $= 0.5''/12.7$ mm).

of the impedance characteristics of acoustic liners under the presence of incident sound and grazing flow, and, in particular, to address the necessary refinements required to ensure that the impedance models can satisfactorily predict the acoustic behaviour of perforate panels in the presence of boundary layers experienced under engine operating and flight conditions. DC flow, normal impedance and grazing flow tests have been performed, resulting initially in improved perforate liner impedance models, which may then be used to help insure that this commonly used low cost design can provide the maximum possible attenuation.

Fig. 18 shows an example of the modelled single layer perforate liner resistance fit to measurements [15] [by P. Murray, P. Ferrante, A. Scofano, Aermacchi S.p.A., Italy, paul.murray@ext.aermacchi.it, pferrante@aermacchi.it, ascofano@aermacchi.it].

4.5. Optimisation of non-uniform liners

The propagation of sound in a cylindrical annular nozzle, in the presence of an uniform axial flow, is studied in the case of impedance walls. The wall impedance may vary circumferentially, or axially, or in both directions [16]. The impedance is represented by Fourier series, and hence is assumed to be a function of bounded variation, allowing continuous or abrupt impedance changes, such as patches. It is shown that the circumferentially non-uniform impedance couples the azimuthal modes, and similarly a longitudinally non-uniform impedance couples the axial modes. The frequencies of the modes are specified by the roots of an infinite determinant, which reduces to its diagonal only in the de-coupled case, of uniform impedance. It is shown that a non-uniform liner can lead to a larger number of duct modes than a uniform liner.

The optimisation of non-uniform linear impedance can be made by: (i) selecting an optimisation criterion, e.g. minimum acoustic energy; (ii) specifying parametric form of impedance, where the parameters can be selected. The example in Fig. 19 concerns a circumferential distribution of specific impedance $Z = Z_0(1 + \varepsilon \cos\theta)$, where the parameters are the real and imaginary parts of ε. The slowest decaying mode ζ for uniform impedance Z_0 is chosen, and the axial decay rate Im(ζ), plotted as a surface. The decay rate of this mode is maximized by largest value of Im(ζ), and the corresponding values of Re(ε) and Im(ε) specify the optimum impedance distribution for this criterion [17] [by L.M.B.C. Campos, J.M.G. Oliveira, Instituto Superior Técnico, Portugal, aero@popsrv.ist.utl.pt].

5. Airframe noise

5.1. Preliminary results on slat-wing overlap variation on aerodynamic performance data and sound radiation

Based on a generic 2D high-lift section represented by a slat and a main-wing, the influence of slat setting variations are investigated with regard to aerodynamic and aeroacoustic responses. The profile section has

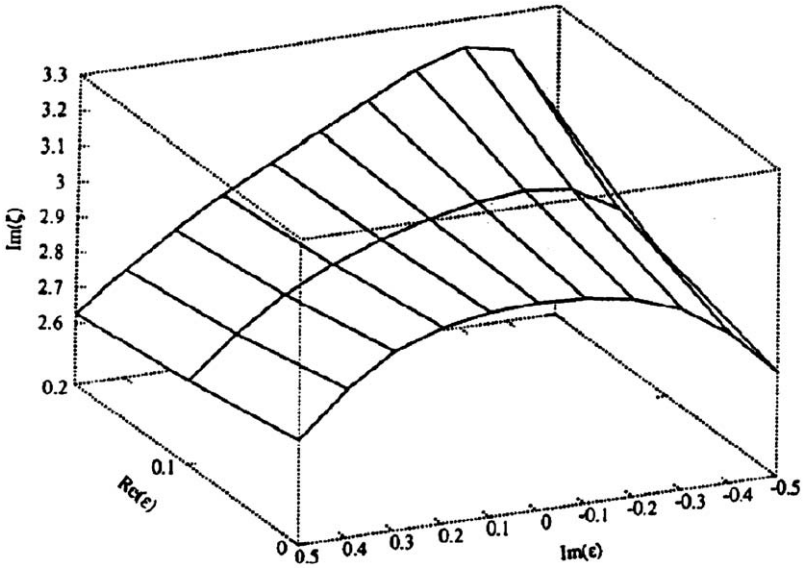

Fig. 19. Axial decay rate for the slowest decaying mode.

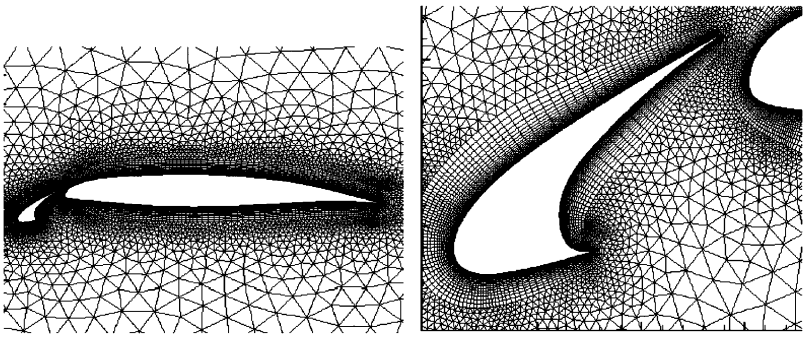

Fig. 20. 2D-Hybrid numerical mesh (approx. 51,500 grid points).

been originally designed to meet the aerodynamic performance data of a real three-element section. Performance data of the baseline section are taken as a reference to judge on the effect of gap variations (overlap = : XRXD = −0.016, −0.0156, −0.015, −0.01, −0.005, increasing magnitude means increasing overlap). The geometry with the underlying CFD mesh is depicted in Fig. 20. Acoustic predictions are done based on the PIANO code [18] using the LEE. A test vortex is injected close to the slat hook into the underlying steady state flow field coming from CFD (2D RANS solution) to investigate the transformation of vortical energy into acoustic sound energy.

In general, reductions in overlap results in a global increase in lift coefficient. For the smallest overlap sizes a gain in lift up to nine counts is predicted for small angles of attack. The significant increase in lift is unfortunately coupled to an also strong increase in drag rise. Thus, the overall performance picture (given by the ratio Cl/Cd) shows that the baseline design can only be reached for certain angles of attack for each of the varied settings. Especially close to the sections design point ($\alpha = 12^{\circ}$) all configurations are less effective than the baseline one (XRXD = −0.0156).

From the rms-directivity (Fig. 21) a global trend can be found:

1. Minor influence of overlap variations on sound radiation towards the sky
2. Significant reduction in sound radiation towards the ground for reduced overlap sizes. The underlying mechanism is the shielding effect of the main wing with respect to radiated sound from the slat trailing edge.

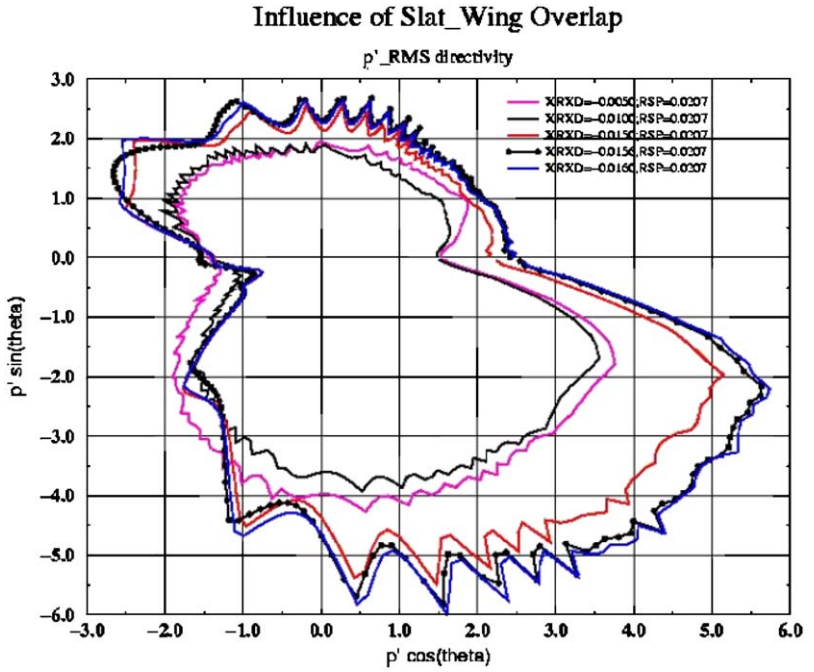

Fig. 21. Impact of slat-wing overlap on rms-directivity.

Some sort of asymptotic behaviour in the reduction of sound radiation towards the ground with decreasing XRXD can be found (no reduction in sound radiation for $\mathrm{XRXD} < -0.0100$).

From the distribution of the PSD (Fig. 22) plotted in the direction $\theta = -18^\circ$ (θ being measured counter-clockwise from the horizontal axis, coordinate system located at upper slat trailing edge) a significant reduction in PSD-level can be found for the slat overlap size $\mathrm{XRXD} = -0.01$ at about 1 kHz. Nearly no difference in the PSD distribution is present for all higher overlap sizes [by R. Emunds, Airbus Deutschland, Bremen, Germany].

5.2. *Slat noise predictions using CAA with stochastic sound sources based on solenoidal digital filtering*

In recent work related to the fast CAA prediction of broadband high-lift noise [19], turbulence field data based on steady RANS computations has been used as an approximate means to characterize the local amplitude and length scales of turbulence in spatially inhomogeneous flows. The computational approach involves CAA techniques to compute sound propagation in inhomogeneous mean-flows in conjunction with stochastic sound sources in the time domain. The mean-flow is determined from steady RANS simulations. The fluctuating right-hand side source term is modelled by a new stochastic particle method (solenoidal digital filtering, SDF), which reconstructs the spatially varying turbulent kinetic energy and length scale of the related steady RANS mean-flow simulation. The convection property of vortical disturbances is included in the model, which is deemed to be important to predict correctly velocity-scaling laws for airframe noise problems. Furthermore, the pseudo-turbulent velocity field from SDF is strictly solenoidal such that spurious sound sources are avoided. The SDF method reproduces target first and second order one- and two-point statistics. In particular, in case of homogeneous isotropic turbulence, it is capable to reproduce exactly the complete second order two-point velocity correlation tensor [19]. The new stochastic method is time and memory efficient and can easily be applied to highly non-uniform mean-flows. Furthermore, it avoids the occurrence of shear de-correlations and resolves broadband spectra continuously. For the considered slat-noise problem, the overall benefit in computational time reaches roughly three orders of magnitude compared to LES. Hence, the

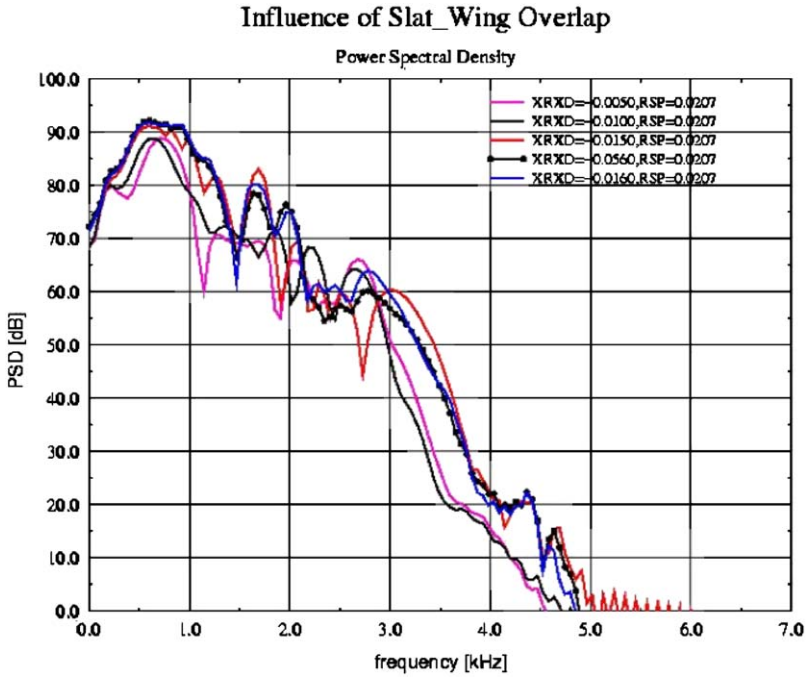

Fig. 22. Impact of slat-wing overlap on power–spectral–density (PSD).

application of the stochastic method to high Reynolds number problems in a design optimization loop becomes feasible.

The unsteady source term and the acoustic pressure field from the SDF source model are presented in Fig. 23. Furthermore, a comparison of the predicted narrow band spectrum (SDF) to that of a related acoustic wind tunnel measurement (AWB) is shown. Almost perfect agreement in the decay of both spectra is achieved. The acoustic field roughly corresponds to that one would expect from a dipole source placed at the slat trailing edge with its axis normal to the slat chord [by R. Ewert, DLR, Braunschweig, Germany].

5.3. *Direct computation of the noise radiated by a high-Reynolds-number 3D airfoil*

The flow around a 3D NACA 0012 airfoil at a Reynolds number of 500,000 and at zero incidence to the flow has been computed by large eddy simulation (LES) in order to obtain directly its radiated acoustic field [20]. The simulation was performed on a parallel computer and made use of low-dissipation and low-dispersion numerical schemes on a fifteen-million-point C-shape curvilinear grid. The grid had a large number of points in the boundary layer in order to describe properly the dynamics of the turbulent features. In this way the unforced transition of the boundary layer around the airfoil from an initially laminar state to a turbulent state before reaching the trailing edge was successfully captured. In particular the location of the transition zone and statistical quantities such as the local pressure coefficient and rms velocity fluctuations were found to be in good agreement with experimental data. The acoustic waves generated by the flow at the trailing edge were calculated directly. As illustrations, snapshots of vorticity and of sound pressure are shown in Fig. 24 [by O. Marsden, C. Bogey and C. Bailly, Ecole Centrale de Lyon, France, Christophe.bogey@ec-lyon.fr].

5.4. *Analysis of A319 flyover airframe noise data*

For the definition of low-noise approach procedures a semi-empirical airframe noise prediction scheme was developed and validated through dedicated flyover noise measurements on an A319 aircraft provided and operated by Lufthansa AG. Noise data were acquired by means of 36 distributed ground microphones to

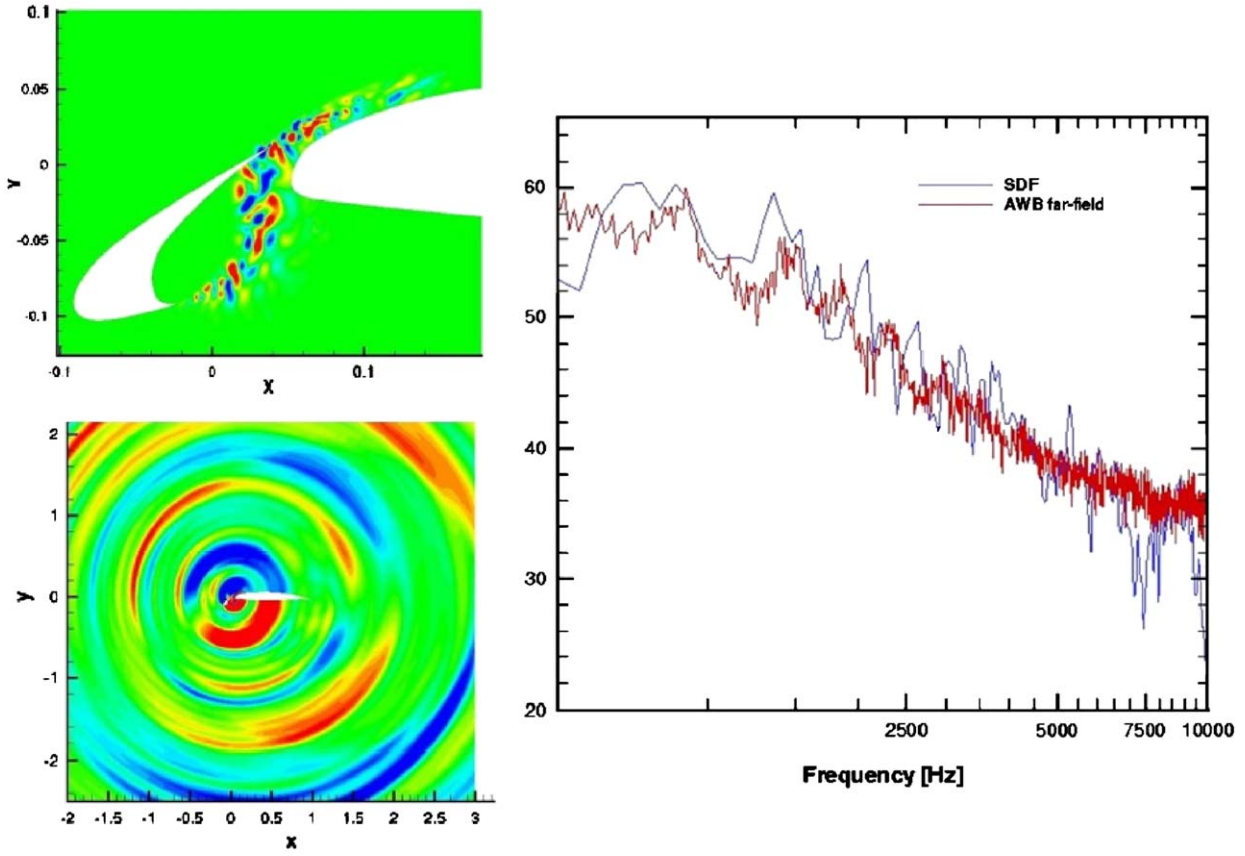

Fig. 23. Fast CAA–SDF slat-noise simulation and comparison with wind tunnel data (AWB).

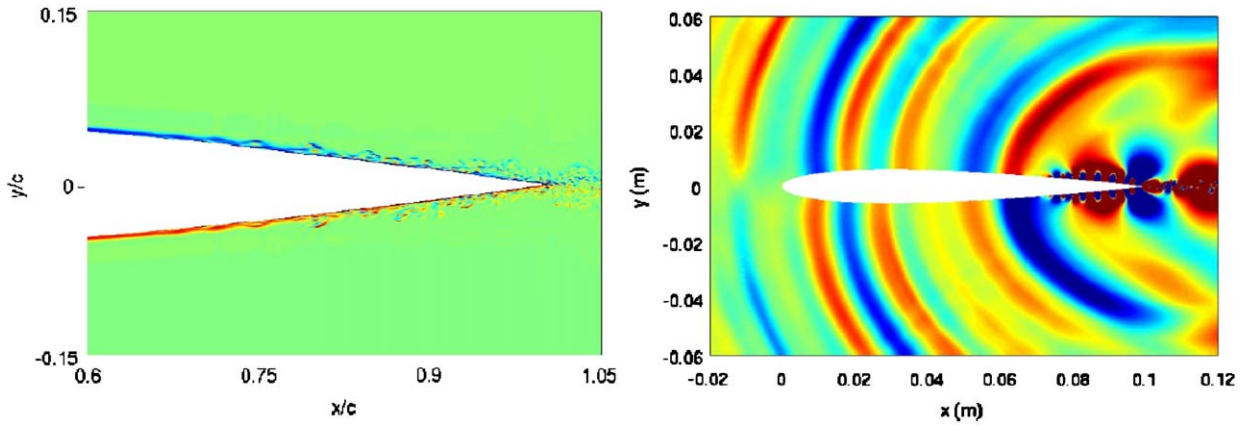

Fig. 24. Large Eddy Simulation of the flow around a 3D NACA 0012 airfoil at a Reynolds number of 500,000 and of its radiated sound field. Left: snapshot of the vorticity field in the boundary layer around the trailing edge, right: snapshot of the pressure field.

acquire the noise carpet, i.e. the noise impact in both flight and lateral directions. The data were corrected for flight (moving source) and propagation effects, thus providing the noise radiation directivity for a stationary source. Flyovers were performed for all different standard flap-settings (with and without gears) and the engines operating in flight-idle. The airframe noise characteristics were extracted through energetic subtraction

of noise levels in cruise configuration. The results show that an 18° slat deflection already causes a noise increase of more than 5 dB. An example of the airframe noise directivity for the full configured aircraft (27° slat and 40° flap deflection) is shown in Fig. 25 for a 1/3-oct. band frequency of 400 Hz and depicts a pronounced maximum in the rear arc due to dominating slat noise in this frequency range [by W. Dobrzynski and M. Pott-Pollenske, DLR, Germany].

5.5. *Acoustic wind tunnel measurements on high-lift devices*

In the framework of the German research project FREQUENZ the Corporate Research Centre, EADS Germany, has performed acoustic wind tunnel measurements on a modified high-lift wing to examine low-noise features at the slat and wing trailing edge (Fig. 26). The experiments aimed at the generation of detailed aerodynamic and acoustic data for validation of computational aeroacoustic methods for noise prediction.

Parametric wind tunnel studies have been performed on high-lift wing with deployed slat over a wide range of angles of attack and various velocities (Fig. 27). Based on an extensive set of far field noise data and microphone-array measurements the effects of flow velocity and aircraft angle of attack on slat noise and radiation characteristics have been determined. Hot-wire measurements have been conducted in cooperation with the Institute of Aerodynamics, RWTH Aachen, in the slat cove region and at the slat trailing edge for selected configurations. On basis of the generated experimental data, slat noise mechanisms have been evaluated and the benefit of different slat cove modifications has been estimated.

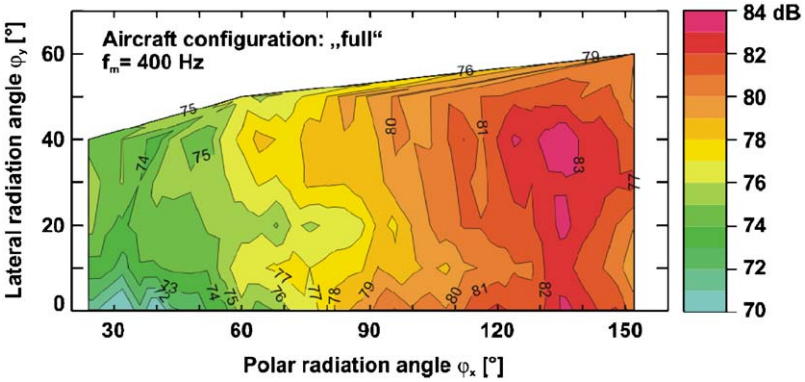

Fig. 25. Example of airframe noise directivity for the A319 in "full" configuration with landing gear retracted.

Fig. 26. Model mounted between plates in the open test section of the wind tunnel (left); bottom view on the wing with deployed slat.

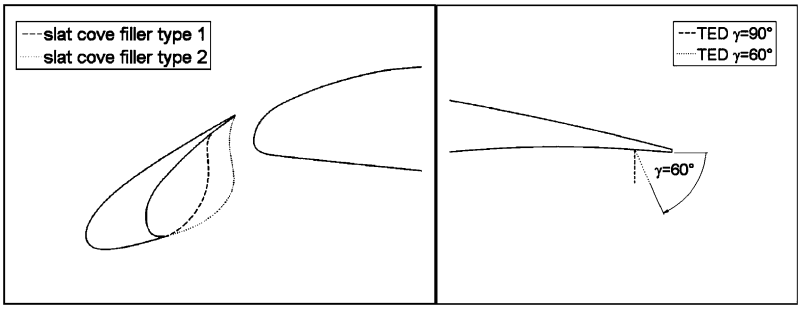

Fig. 27. Shape of two different slat cove fillers (left); position of two different Mini trailing edge devices (TED) at the main wing trailing edge.

In a second study, different trailing edge devices have been investigated by acoustic measurements and supported by aerodynamic data. Parametric dependencies have been evaluated and the gain of the trailing edge modifications has been summarized.

Supplementary particle image velocimetry (PIV) measurements have been performed at the slat cove region and at the trailing edge device for selected configurations in cooperation with the Institute of Aerodynamics, RWTH Aachen, and AIRBUS Deutschland, Aerodynamic Design & Data [by A. Kolb, M. Grünewald Corporate Research Centre, EADS Germany, alexander.kolb@eads.net, michael.gruenewald@eads.net].

6. Combustion noise

6.1. Measurements of combustion noise

Combustion noise experiments performed at the DLR Institute of Propulsion Technology have shown strong evidence that entropy noise is the major source of external combustion noise of aero engines. Entropy noise is generated in the outlet nozzles of combustors. Low frequency entropy noise—which was predicted earlier in theory and numerical simulations—was detected in a generic combustion chamber. In addition to this, another noise generation mechanism at higher frequencies (above 1 kHz in the experiments) was discovered, which is presumably of even higher relevance to jet engine noise. This unexpected effect can be explained by the interaction of small-scale entropy perturbations (hot spots) with the strong pressure gradient in the turbulent flow of the outlet nozzle. The direct combustion noise of the flame zone seems to be of minor importance for the external noise radiation. The above findings were supported by additional model experiments where the entropy waves were generated by electrical heating. Fig. 28 shows the broad-band entropy noise as function of the Mach number in the outlet nozzle of a combustion chamber [by F.Bake, U. Michel, I. Röhle, DLR Institute of Propulsion Technology, Engine Acoustics Berlin].

6.2. Acoustic perturbation equations for jet and combustion noise

Acoustic perturbation equations (APE) are used to compute the sound field radiated from high Mach number jets and turbulent diffusion flames. Both cases are simulated using a hybrid method in which the fluid mechanical solutions of jets and flames are carried out by LES while the acoustic simulation uses the APE system, which was proposed by Ewert and Schröder to calculate, e.g., airframe noise [21]. The appealing properties of the APE system, i.e., the capability of simulating acoustic wave propagation within a non-uniform mean flow while it is stable for arbitrary mean flows, are the reason for using this system for the acoustic simulation instead of the LEE.

The APE system has been extended to the APE for reactive flows (APE-RF) to examine the acoustic source mechanism within a reactive flow such as the turbulent diffusion flame. Rearranging the conservation equation of mass and momentum for a multicomponent fluid and subtracting the averaged equations, respectively, such that the left-hand side results in the original APE system leads to the equations for the

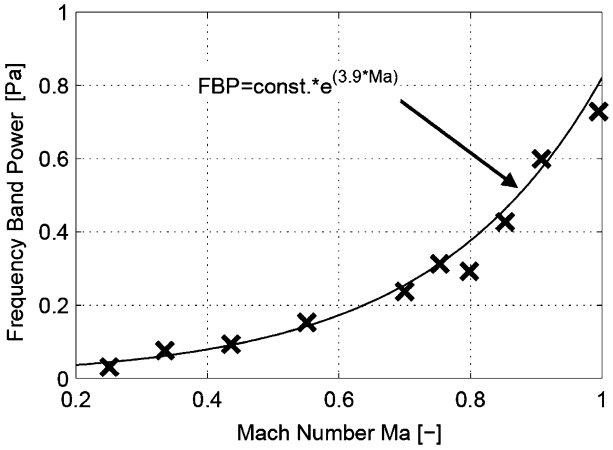

Fig. 28. Increase of frequency band power of entropy noise (1–5 kHz) with the Mach number of a turbulent nozzle flow with temperature inhomogeneities of approximately ± 10 K.

perturbation density and velocity components of the APE-RF system. Additionally to these two equations, a pressure-density relation has to be included to close the system whose right-hand side (RHS) is zero if only isentropic flows are considered. However, in the case of combustion this source term cannot be neglected. It is this RHS of the pressure-density relation, which includes the source dominating the excitation of acoustic waves in combustion noise. Furthermore, it has been discussed in [22] that the experimental and numerical comparison of the intensity distribution showed the heat release rate per unit volume, which is expressed via the total time derivative of the density, to represent the major source term in the APE-RF system when combustion noise is analyzed.

Moreover, the noise prediction by the hybrid LES/APE method has been successfully applied to highly compressible low- and high-Reynolds number jets [23]. The proper noise characteristics of such Reynolds number jets were obtained for the downstream and sideline noise showing the correct noise generation mechanisms to be determined. The LES/APE solution has been less susceptible to the size of the source region compared with acoustic analogies based on conventional wave equations such as the Ffowcs-Williams Hawkings approach. Moreover, the dominant source term in the APE formulation for cold jets has been shown to be the Lamb vector. From these findings, a further reduction in the total memory of the LES data for the acoustic simulation is possible [by E. Gröschel, T. Ph. Bui, M. Meinke and W. Schröder, Institute of Aerodynamics, RWTH Aachen University, Germany, e-mail: e.groeschel@aia.rwth-aachen.de].

7. Helicopter noise

7.1. Noise reduction through active blade control using servo flaps

A four-bladed BK117 rotor of advanced geometry has been equipped with small trailing edge servo flaps (Fig. 29) for flight testing of Active Blade Control—a powerful tool to alleviate typical problems of helicopter flight such as impulsive noise (Blade slap or BVI), vibrations and dynamic loads. First flight tests with still open loop control laws have produced about 90% vibration and about 3–4 dB BVI noise reduction. Closed loop tests addressing additionally manoeuvre load alleviation, unbalance compensation, and blade lead-lag damping are under preparation. In order to increase efficiency and robustness of this technology, a five-bladed bearing less main rotor with improved servo flaps is under development.

The research activities are promoted by the partners ECD, EADS-CRC, DLR and ONERA [by V. Kloppel, Eurocopter Deutschland GmbH, Germany].

Fig. 29. Flight tests on a full scale helicopter equipped with blades using servo flaps for active blade control.

7.2. Acoustic and aerodynamic test results from HeliNOVI main rotor/tail rotor/fuselage test in DNW

The European HeliNOVI (Helicopter Noise & Vibration Reduction) project is part of the continuing effort within EU towards improving the understanding of tail rotor noise reduction and vibration reduction technology by means of a comprehensive investigation of main rotor (MR)/tail rotor (TR) interaction noise and rotor induced vibrations through both theory and experiment [24,25]. A comprehensive experimental program within HeliNOVI was launched employing 40% geometric and dynamic scaled helicopter wind-tunnel model. The model was well equipped with densely instrumented MR and TR as well as a lightly instrumented fuselage. In order to improve the understanding of the effect of the MR wake on the TR inflow, a three-component flow visualization and flow velocity measurement, by means of PIV, were also employed on planes near TR inflow and outflow region parallel to the free stream. The acoustic signal was measured by the inflow microphone array (16 Mics) mounted on a traverse. Besides the conventional measurement techniques, a 140-microphone out-of-flow phased array was applied to locate and quantify the different noise sources on the model. The whole wind tunnel test was divided into two parts, an aeroacoustic test and a vibration test. The goal of the aeroacoustic tests was to investigate (1) the importance of TR noise for different flight conditions (2) MR/TR interaction noise, and (3) TR noise reduction concepts. Fig. 30 gives an overview of the test set up and DLR test rig as well as inflow and outflow microphone system in this wind tunnel. One example of flow visualization from one PIV window for 12° climb at 33 m/s case is given in Fig. 31. The tested configuration in aeroacoustic part address a number of noise reduction techniques; (1) TR sense of rotation (NACA 0012 TR used), (2) Variation of position between MR and TR (S102 TR used), (3) Variation of rotor rotational speed. The flight conditions covered include level, climb, and descent flight at various flight speeds. The test results indicate that tail rotor noise is most important for climb and high-speed level flight. Furthermore, it has been found that MR/TR interactions only have a small effect on the overall noise levels. After the reduction of rotor tip speed, the most efficient TR noise reduction concept involves changing the TR sense of rotation from 'advancing side down (ASD)' to 'advancing side up (ASU)'. As an example of the test results, the mean dBA value (averaging over measured area or over all microphone positions) as a function of three different flight conditions is given in Fig. 32 for two different TR rotational directions; ASD and ASU. When compared to TR in ASD mode, a noise reduction of more than 5 dBA is observed for the 12° climb and 60 m/s level flight conditions in ASU mode. There is no change on overall noise radiation for 6° descent while MR BVI noise is the dominant noise source [by J. Yin, DLR Braunschweig, Germany jianping.yin@dlr.de].

7.3. Aeoracoustic modelling of BVI

The aeroacoustic analysis of helicopter rotors in BVI conditions requires the availability of an aerodynamic solver for the blade pressure prediction that is capable to capture blade-vortex interaction effects. A direct panel method based on a novel boundary integral formulation for the velocity potential has been developed and applied to helicopter rotors experiencing blade–vortex interaction (BVI) [26]. It avoids the numerical

Fig. 30. HeliNOVI test set up for aeroacoustic test.

instabilities arising in the standard direct panel method in case of blade/wake impingement. This aerodynamic solver yields a unified approach for the calculation of free-wake evolution and blade pressure field. It is fully 3D, includes body thickness effects, and can be applied to blades with arbitrary shape and motion. This formulation has been successfully applied to the aeroacoustics of helicopter rotors in descent flight [26] [by M. Gennaretti, Giovanni Bernardini, University Roma "Tre", Italy, m.gennaretti@uniroma3.it].

8. Wind turbine noise

8.1. Acoustic array measurements on a full scale wind turbine

Acoustic array measurements were performed on a three-bladed GAMESA G58 wind turbine with a rotor diameter of 58 m (Fig. 33). The goal was to characterize the noise sources on this turbine, and to verify whether aerodynamic noise from the blades is dominant. In order to assess the effect of blade roughness, one blade was cleaned, one blade was tripped, and one blade was left untreated. The acoustic array consisted of 152 microphones mounted on a horizontal wooden platform ($15 \times 18\,m^2$), which was positioned about one rotor diameter upwind from the rotor. Apart from the acoustic measurements, a number of turbine parameters were monitored, such as wind speed, power, turbine orientation, rev/min, and blade pitch angle. Altogether more than 100 measurements were taken at wind speeds between 6 and 10 m/s. Two array-processing methods were used to characterise the noise from the turbine. First, the noise sources in the rotor

Fig. 31. One example of flow visualization from one PIV window for 12° climb case (wind comes from right side).

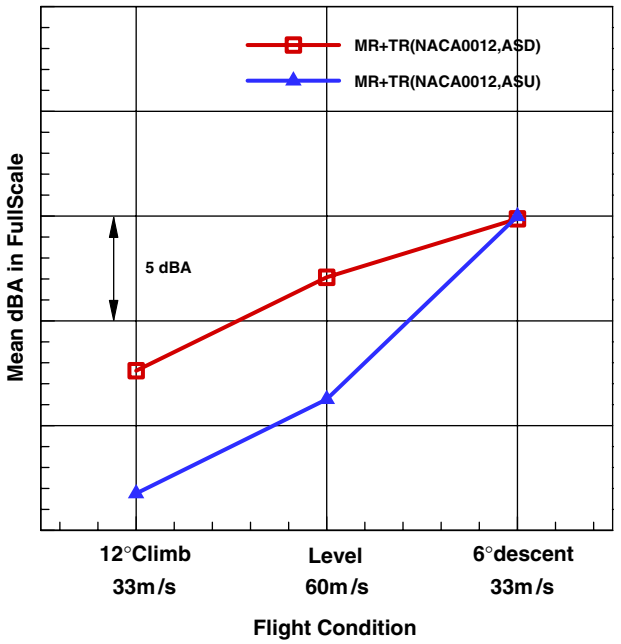

Fig. 32. Mean dBA value as a function of typical flight condition for TR in ASD and ASU mode.

plane were localised using conventional beam forming. These results clearly show that, besides a minor source at the rotor hub, practically all noise (radiated to the ground) is produced during the downward movement of the blades. The noise is produced by the outer part of the blades, but not the very tip, while blade noise levels scale with the fifth power of the local flow speed. The second processing method was based on rotating scan planes to localise the noise sources at the individual blades. It turns out that the tripped blade is significantly noisier than the clean and untreated blades, which strongly indicates dominating trailing edge noise, rather than noise due to inflow turbulence noise. The similar noise levels for clean and untreated blades support the assumption that the untreated blade was aerodynamically clean [27] [by S. Oerlemans, NLR, The Netherlands].

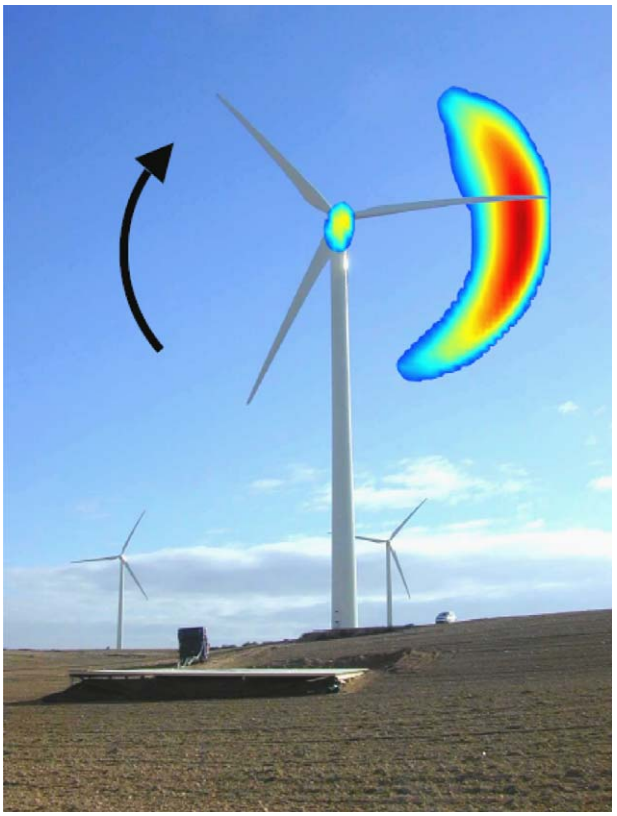

Fig. 33. Test set-up with G58 turbine and microphone array platform. The noise sources in the rotor plane (averaged over several rotations) are projected on the picture.

9. Techniques and methods in aeroacoustics

9.1. High-order difference approximations for aeroacoustics

Strictly stable high order finite difference approximations have been employed to discretize the 2D compressible Navier–Stokes equations. The approach has been verified for the Karman vortex street behind a circular cylinder and the aeolian tones emitted by vortex shedding from the cylinder. Free stream Reynolds and Mach numbers of $Re = 150$ and $Ma = 0.1$ and 0.2, respectively, have been considered. The directly computed Strouhal numbers, average drag coefficients, amplitudes of lift and drag coefficients, and fluctuation pressure contours and amplitudes are in excellent agreement with reference solutions [28,29] [by B. Müller, Uppsala University, Bernhard.Muller@it.uu.se].

9.2. Accuracy of hybrid prediction techniques for cavity flow noise applications

Nowadays, a large variety of different hybrid approaches exist differing from each other in the way the source region is modelled; in the way the equations are used to compute the propagation of acoustic waves in a non-quiescent medium; and in the way the coupling between source and acoustic propagation regions is made. The research carried out at the department of mechanical engineering at the K.U. Leuven intends to make a comparison between some commonly used methods for aero-acoustic applications [30]. As application, the aerodynamically generated noise by a flow over rectangular cavities is investigated, where a flow-induced oscillation mode is responsible for a tonal noise generation [31]. Source domain modelling is carried out using a second- and fourth-order finite-volume LES. Propagation equations, taking into account convection and

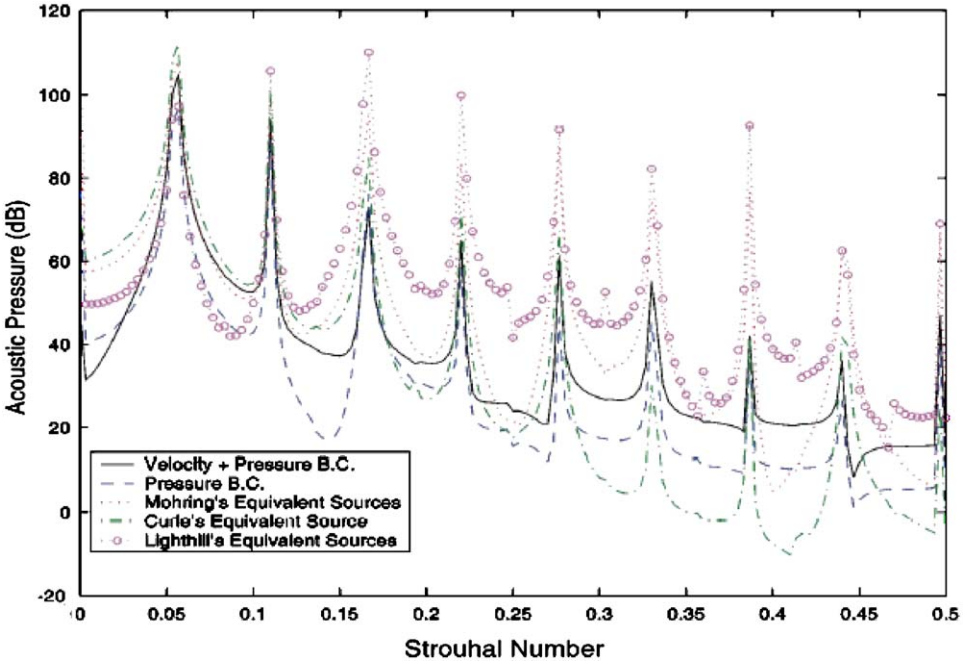

Fig. 34. Acoustic pressure spectrum of different hybrid methodologies for cavity noise application.

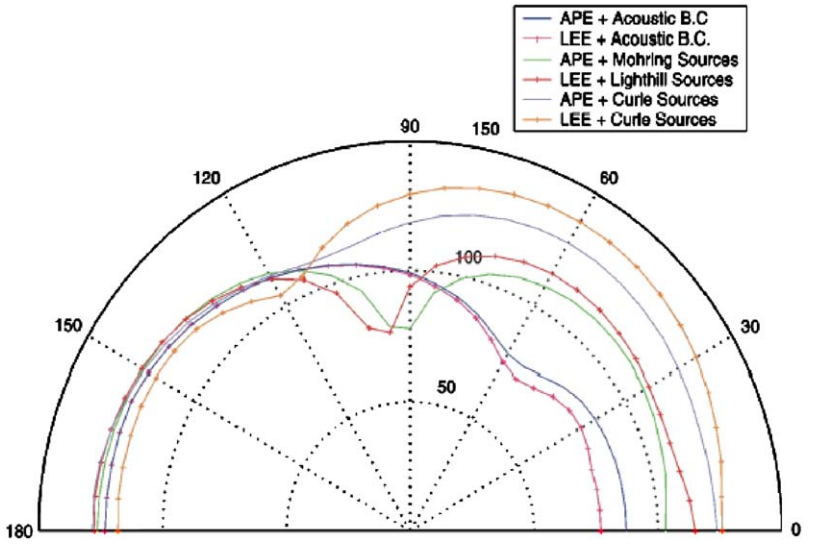

Fig. 35. Directivity of the second Rossiter mode for different hybrid methodologies.

refraction effects, based on a high-order finite-difference formulation and a quadrature-free discontinuous Galerkin implementation of the LEE and APE are compared with each other using different coupling methods between source region and acoustic region (Figs. 34 and 35). Conventional acoustic analogies and Kirchhoff methods are rewritten for the different propagation equations and used to obtain near-field acoustic results. The accuracy of the different coupling methods and their sensitivity to the LES-modelling is investigated [32]. In this way, the research aims at giving more insight in the accuracy and practical use of different hybrid CAA techniques to predict the aerodynamically generated sound field [by W. De Roeck, Katholieke Universiteit Leuven, Leuven, Belgium, wim.deroeck@mech.kuleuven.be].

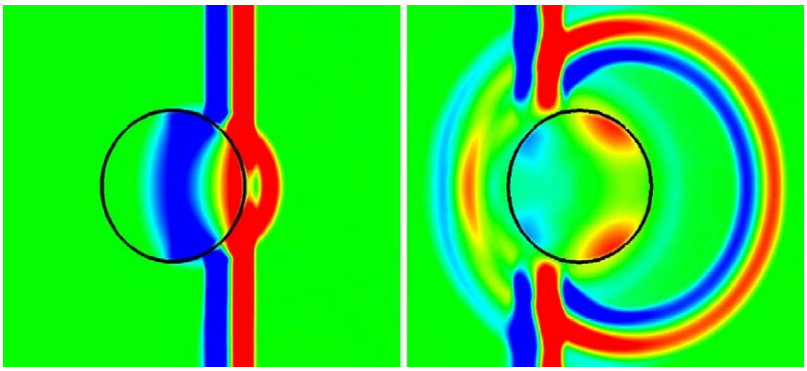

Fig. 36. Plane wave scattering by a fluid bubble of diameter D. External fluid (density, sound speed, heat ratio): $\rho_e = 1$, $c_e = 1$, $\gamma_e = 1$. Inner fluid: $\rho_i = 2.6, c_i = 2.667, \gamma_i = 18.49$.

9.3. Object-oriented discontinuous Galerkin LEE solver

Discontinuous Galerkin (DG) methods are becoming more and more popular in the Computational AeroAcoustics (CAA) community for the discretization of the LEE.

An object-oriented implementation of the DG method is well suited for high-order CAA simulations involving complex geometries, since the discretization of the governing equations can be managed in a symbolically uniform way regardless the shape of the volume cell: each cell-object has its own topological properties that can be calculated once and stored for successive calculations. Not only geometrical properties but also physical properties (base flow, source terms, etc.) can be related to the cell-object. In this environment, is quite easy, for instance, to simulate acoustic transmissions through fluids with different impedance and complex interfaces such as flames, or to integrate heat release models for thermoacoustic simulations. For the above reasons a DG solver is currently under development at the Italian Aerospace Research Center, under the project CAST funded by the Italian Aerospace Agency. The main goal of this project is to predict the acoustic loading on advanced launcher vehicles during lift-off. Furthermore, feasibility studies have been undertaken to investigate the acoustic propagation in multiphase flows. An example is shown in Fig. 36 where a plane wave is scattered by a cylindrical bubble filled with a fluid in pressure equilibrium with the surrounding fluid, but with different temperature, density and specific heat ratio [by M. Genito, V. Botte, D. Casalino, CIRA, Italy, m.genito@cira.it, v.botte@cira.it, d.casalino@cira.it].

9.4. Time domain propagation, attenuation and radiation modelling

MESSIAEN is an EU funded sixth framework program, which focuses on the development of a time domain version of the ACTRAN noise propagation and radiation code (ACTRAN DGM). The time domain version solves the linearised Euler equations with a quadrature-free discontinuous Galerkin method (DGM) on unstructured grids. The code is intended to significantly reduce computation time for large size 3D nacelle aeroacoustic propagation and radiation problems. Fig. 37 presents some of the first check evaluations, performed by Aermacchi, which demonstrate good agreement between the existing frequency based ACTRAN TM and ACTRAN DGM. The project is coordinated by Free Field Technologies (Belgium) with partners Airbus, Rolls Royce, Turbomeca, Liebherr, Aermacchi, UCL, ISVR, TUE, Vibratec, ODS [by P. Murray, P. Ferrante, Aermacchi S.p.A., Italy, paul.murray@ext.aermacchi.it, pferrante@aermacchi.it].

9.5. Nonlinear acoustic solver: a general approach for industry relevant cases

Due to customer and public-driven demand for quieter vehicles, a joint effort has been carried out in the last few years between Metacomp Technologies Inc., and Centro Ricerche FIAT, in order to develop a prediction tool that is general enough to cover the variety of vehicle-associated aeroacoustic phenomena, yet efficient

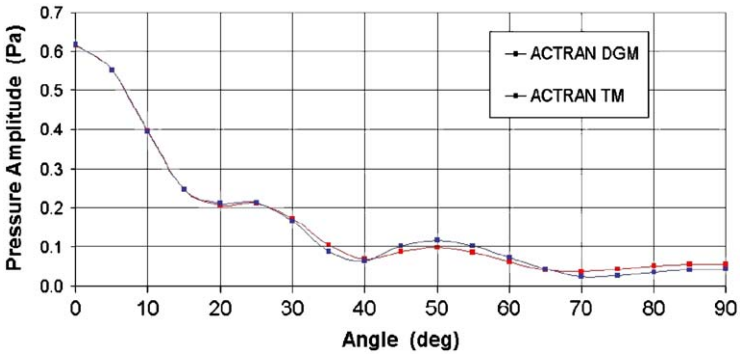

Fig. 37. ACTRAN TM vs DGM Calculations for a Hard-Walled 2D Duct (@2000 Hz).

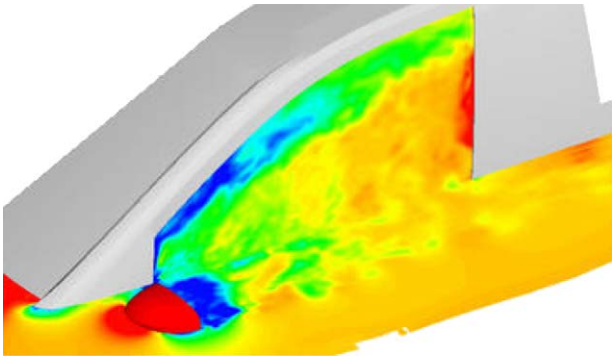

Fig. 38. Instantaneous pressure field over the window and in the wake of the mirror (NLAS simulation).

enough to be compatible with design-process time constraints. A key method at the heart of Metacomp Technologies' CAA++ suite is a novel, nonlinear acoustics solver (NLAS), which provides some interesting advantages over traditional methods, such as LES or the use of LEE. General-purpose noise-prediction methods are expected to handle increasingly complex geometries and a substantial range of Reynolds number and physics, including broadband, fine-scale turbulence-related noise, as well as discrete tones arising from coherent flow structures. The NLAS achieves these goals using an advanced, anisotropic stochastic source reconstruction model, whose energy spectrum does not impinge on resolved-scale disturbances. Using the NLAS, acoustic simulations can be achieved with less near-wall mesh resources than either direct numerical simulation (DNS), LES, or more recent hybrid RANS/LES methods [33]. The use of scale-separated disturbance equations with established turbulence statistics and self-tuning absorbing-layer outer boundary conditions also enables detailed acoustic simulations to be performed in a relatively limited computational domain.

CRF has applied this method to the simulation of several aeroacoustic phenomena in real car configurations, such as noise from the A-pillar vortex and side mirror, buffeting of open sun-roofs, noise from resonant cavities and noise from the ventilation system (an example, with comparison against measured data with flush mounted microphones is shown in Figs. 38 and 39) [34]. The method has also been employed in Metacomp for applications in the aeronautical field, like the noise prediction for a high-lift wing configuration (Fig. 40) [by E. Ribaldone (CRF, Italy) e.ribaldone@crf.it, P. Batten (Metacomp Technologies, Inc., US) batten@metacomptech.com].

9.6. *Investigation of aeroacoustic sources by synchronized PIV and microphone measurement*

Microphone-Array measurements or near-field acoustic holography yield only the location of sources but no information about the source mechanisms. The idea is to combine acoustic measurements in the far field

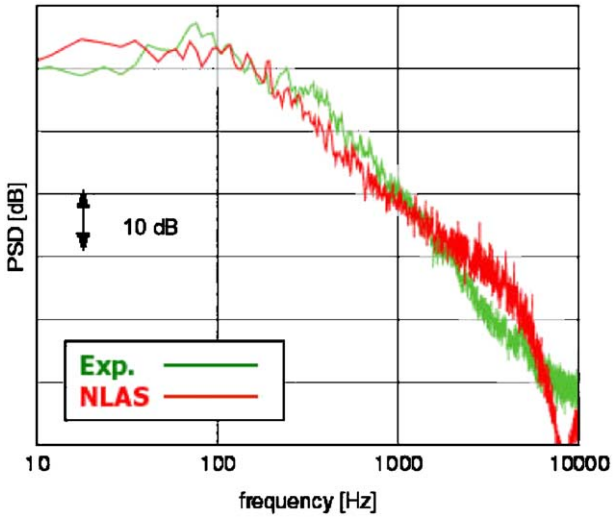

Fig. 39. Comparison of predicted and measured spectra in a point on the window.

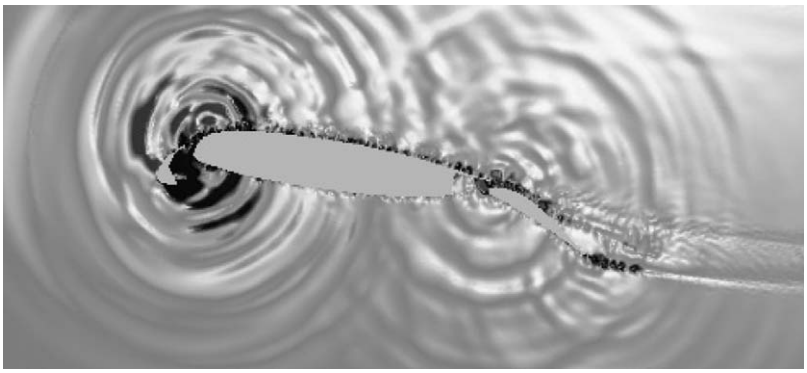

Fig. 40. NLAS prediction of noise from high-lift trap wing configuration.

with PIV in the source region, and to obtain by such measurements more detailed information about the sources.

The flow around a cylinder was chosen as a simple test case to check the feasibility of combined velocity field and pressure measurements. The PIV covered a field directly downstream of the cylinder and the pressure was measured by a single microphone further downstream and far outside of the cylinder wake. The cross correlation between the acoustic pressure and the vorticity fluctuations in the near field were calculated using 5000 PIV recordings.

Fig. 41 shows the resulting cross correlation coefficient $R_{\omega p}$ for zero delay between pressure and vorticity in the case of 20 m/s free stream velocity and $d = 14$ mm cylinder diameter. The coefficient $R_{\omega p}$ is normalized using the standard deviation of the pressure and the maximal standard deviation of the vorticity in the whole measurement area. The plot indicates the regions in the near field with the strongest covariance between the local vorticity and the far field pressure. The maximum magnitude of 0.15 means that, 15% of the vorticity and pressure fluctuations were correlated in the respective point. The amplitude of the cross correlation coefficient at one point in the x,y-plane fluctuates over the delay time in a sine type oscillation with the frequency of 264 Hz which corresponds to a Strouhal number of $St = 0.18$.

The result shows that the calculation of the cross correlation between far field pressure and vorticity obtained by PIV is feasible. In the present case a statistics based on 5000 PIV recordings appeared to be

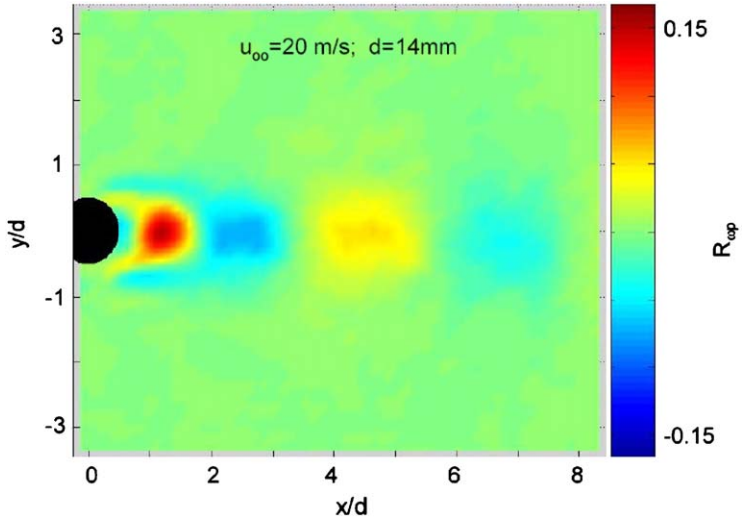

Fig. 41. Instantaneous distribution of the normalized cross correlation coefficient $R_{\omega p}$.

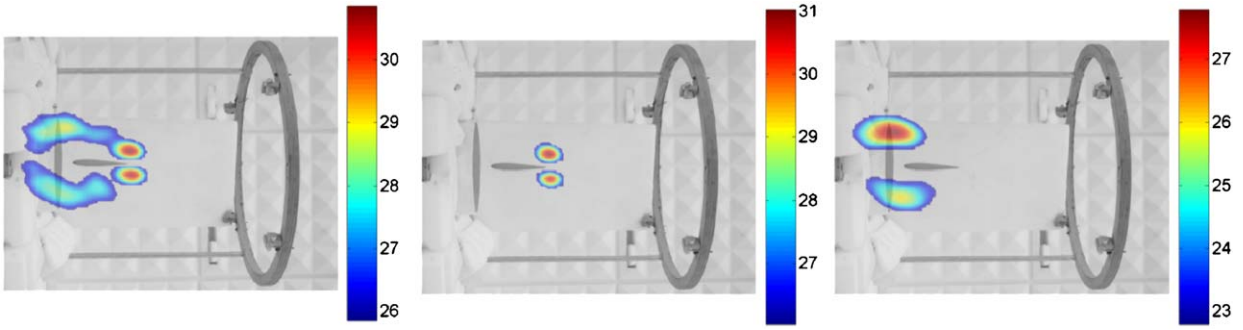

Fig. 42. Sound sources at a NACA0012 airfoil in the low speed aeroacoustic wind tunnel ($Ma = 0.11$), SPL at microphone array in dB for the 8 kHz octave band. Left: conventional beam-forming result, centre: first component of orthogonal beam-forming (trailing edge noise), right: second component (unwanted noise, probably from the wind tunnel).

sufficient to obtain cross correlation values with reasonable signal to noise ratio. Furthermore, the tests show that by the combination of PIV and acoustic measurement the flow structures in the near field which are related to the sound in the far field can be identified [by L. Koop, K. Ehrenfried; DLR, Germany, K. Käpernick, RollsRoyce Germany, lars.koop@dlr.de].

9.7. *Orthogonal beam-forming technique for separation of sound source mechanisms*

A microphone array and conventional beam-forming techniques may be used to map relative sound pressure contributions from aeroacoustic sound sources. Thus, it is possible to localize and quantify these sound sources experimentally but no information is given on how the sound pressure contributions relate to different source mechanisms. Utilizing the orthogonality of the sound fields from different source mechanisms, a novel algorithm for processing the microphone output signals is able to separate these contributions. This orthogonal beam-forming technique may be applied to the separation of the sources of interest from unwanted noise (Fig. 42). Another application is to detect minor sound sources that would be covered by noise when using conventional beam-forming algorithms. The algorithm was developed by the consulting firm Gesellschaft für Akustikforschung Dresden mbH in cooperation with the universities of Cottbus and Dresden

Fig. 43. Radiation of the spinning mode (18,1) from a scarfed intake with segmented acoustic treatment. The dimensionless impedance values are: ■ ▧ ▨ $Z=\infty$ ■ $Z=(2,-2)$ ▨ $Z=(2,-1)$.

and is used within the AcoustiCam microphone array system [35] [by E. Sarradj, Brandenburgische Technische Universität, Germany, ennes.sarradj@tu-cottbus.de].

9.8. Predictions of fan noise radiation from aeroengine intakes with segmented wall impedance

The Green's function discretization (GFD) method is an alternative to continuous Galerkin method for the discretization of the wave equation for the harmonic acoustic potential ϕ. It is based on the use of elementary solutions of the locally uniform wave equation to compute the discretization coefficients of a generic spatial derivative of ϕ in a finite difference scheme for unstructured grids with arbitrary stencil. Since the discretization coefficients depend on the local stencil, local mean flow and acoustic wavenumber, accurate numerical solutions can be achieved with only 3–4 nodes per wavelength [36]. The GFD method has been recently used to compute the fan noise transmission through and radiation from a scarfed aeroengine intake at the Helmholtz number (based on the outer intake radius) of *20* [37]. The intake configuration is shown in Fig. 43 where colours denote different patches of acoustic impedance, liners and splices included. The transmission of the spinning mode (18,1) is computed for various combinations of the wall impedance [by P. Di Francescantonio STS, Italy (pdifra@mclink.it), and D. Casalino, CIRA Italy (d.casalino@cira.it)].

9.9. Frequency-domain solution of convected wave equations

A fast numerical method, developed for the solution of the original Lighthill's wave equation [38], has been extended to the convected wave equation valid for non-uniform mean flows [39]. Assuming harmonic time dependence, the wave equation is solved in the frequency domain on an unstructured mesh. For each wavenumber, an associated convected Helmholtz problem, with the corresponding inhomogeneous forcing term, is solved by means of a preconditioned GMRES technique. The technique has proved to be fast and accurate for high frequency modes. The main advantage with respect to existing techniques is the ability of dealing with generally shaped boundaries. Moreover, the frequency-domain discretization approach makes possible to treat each wavenumber separately. This property is particularly useful for design optimization calculation, for example in the case of the cut-on/cut-off spinning modes in aircraft turbofan aeroacoustic analysis.

Two classes of high-order difference schemes have been applied to the solution of the LEE [40]. The first one is a class of centered non-compact high-order and optimized finite-difference methods, proposed in the literature for the simulation of high-frequency linear wave phenomena, with a seven-point stencil. The numerical scheme is composed by a skew-symmetric part and a symmetric part. The classical DRP schemes are a particular case of this wider family. The second class is formed by the upwind WENO schemes. Numerical tests have been performed comparing a fourth-order accurate centered scheme, the fourth-order

DRP scheme, and a fourth-order WENO scheme. All the schemes have comparable computational cost. Different multiblock grid topologies, with grid line slope discontinuities and grid stretching, have been tested. The metric discontinuities induce parasitic oscillations into the solution, which can be damped by adding a numerical dissipation, based on the fourth- and sixth-order derivatives, in the case of the centered and DRP schemes, while the WENO schemes are intrinsically stable. The numerical tests showed a better performance of the WENO scheme with respect to the others [by A. Renzo, Politecnico di Torino, Italy, renzo.arina@polito.it].

9.10. Sound propagation in axisymmetric vortex flow

The propagation of sound is studied in a cylindrical vortex with velocity decaying as the inverse of the radius (potential vortex) allowing also for a uniform axial velocity. This can be used also to study sound propagation in a cylindrical or annular duct, with an uniform axial flow and swirl velocity inversely proportional to the radius. The exact solution of the problem is obtained by two overlapping asymptotic expansions: (i) one centered on the axis, where it has a singularity specified by the Doppler shift, (ii) another centered at infinity, where the tangential velocity decay to zero, leading asymptotically to a cylindrical waves. The two solutions can be used to calculate the natural frequencies and mode shapes. For example, Fig. 44 shows the amplitude and phase of the three radial modes, for the azimuthally wavenumber $m = 1$, in a rigid cylindrical duct, with given axial and tangential (at the wall) flow Mach numbers and dimensionless frequency [41] [by L.M.B.C. Campos & P.G.T.A. Serrão, Instituto Superior Técnico, aero@popsrv.ist.utl.pt].

9.11. Turbulence modelling for aeroacoustic noise sources extraction

The Fluid Mechanics department is currently developing a fast solver for turbulent constant density flows. The code is based on a hybrid finite element/spectral discretization in space, which leads to an interesting decomposition of the large-system coupling the unknowns.

We are interested in the evaluation of turbulence models for aeroacoustic noise sources extraction. The noise sources are extracted from the incompressible flow field using the classical Lighthill analogy. We are currently testing on moderate Reynolds number flows the ability of the flow solver to produce a correct noise field, which could be transferred to an acoustical solver for sound propagation purposes. At this level, turbulence does not play a significant role, and we may test the extraction tools and compare the results of different approaches without the influence of a turbulent model.

Fig. 45 illustrates the comparison between flow streamlines of a jet at Reynolds 1500 (left) and one component of the Lighthill tensor (right).

The next step will be the evaluation of the accuracy of the Lighthill tensor for the acoustic solver. This involves the evaluation of the extension and the localization of the source region based on flow quantities. Acoustic mesh generation will be optimized to bring the relevant flow quantities to the acoustic level [by Y. Detant, G. Degrez, Université Libre de Bruxelles, Belgium, ydetandt@ulb.ac.be, gdegrez@ulb.ac.be].

10. Miscellaneous topics

10.1. Aircraft interior noise

10.1.1. Advanced hybrid simulation of interior noise

Within 2005 EADS highlights on interior acoustics research is mainly dedicated to the simulation of advanced hybrid simulation procedures. Using this procedure the fuselage structure is modelled using structural FEM, whereas excitation from and radiation into are modelled as statistical subsystems or excitation. Using this modelling the sound transmission due to excitation via turbulent boundary layer and acoustic fields can be calculated at reasonable time and high frequency ranges.

In Fig. 46 the result using this method is shown for calculating the transmission loss of two comparable fuselage structures made out aluminium and one built by monolithic CFRP. Furthermore as one measure to overcome the classic mass law limit in the low frequency domain, active shock mounts (Fig. 47) were applied

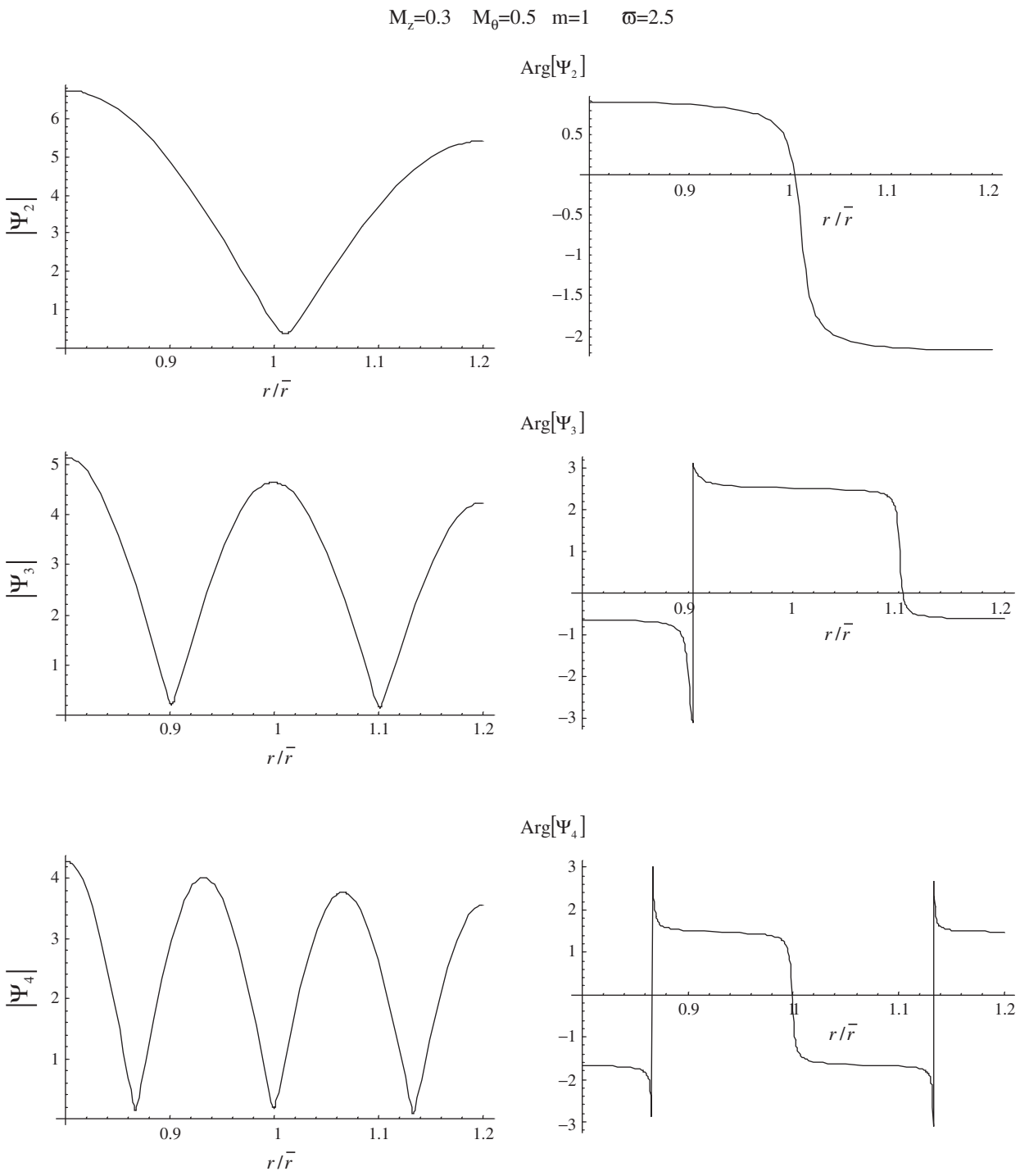

Fig. 44. Amplitude (left) and phase (right) of the acoustic potential eigenfunctions Ψ_n radial $n = 2$ (top), $n = 3$ (middle), $n = 4$ (bottom) for integral azimuthal wavenumber $m = 1$.

to reduce especially the harmonic buzz saw noise. In laboratory results using generic AC double wall structure excited by realistic levels a reduction of 10.4 dB in the 80 Hz third octave band could be achieved [42] [by A. Peiffer, S. Tewes, S. Brühl, EADS Corporate Research Centre, Alexander.peiffer@eads.net].

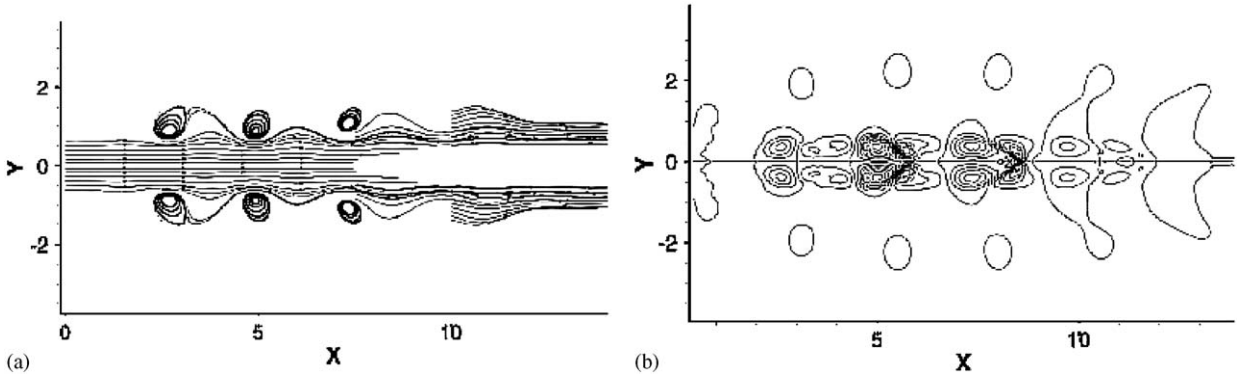

Fig. 45. Simulation of a jet flow at $Re = 1500$. (a) Flow lines and (b) Cross Lighthill tensor component.

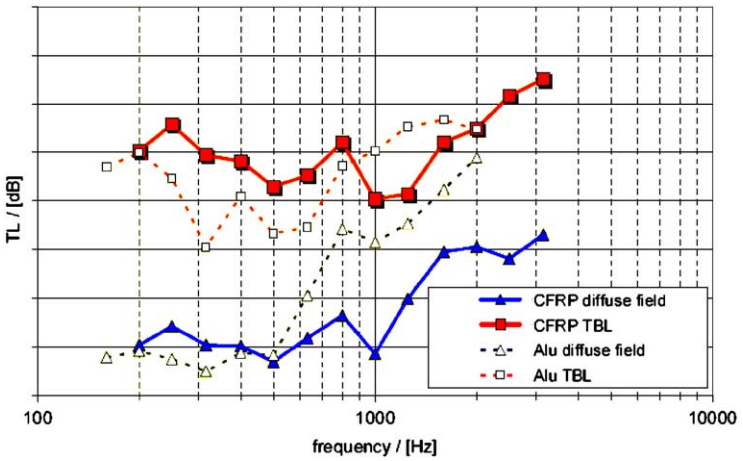

Fig. 46. Comparison of transmission loss due to typical turbulent boundary layer and diffuse field excitation of CFRP and metallic fuselages.

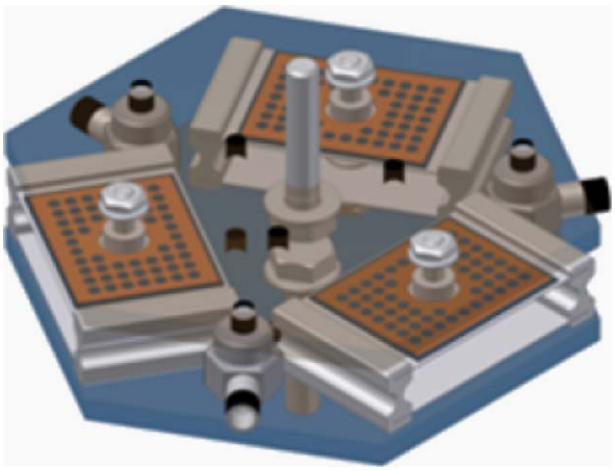

Fig. 47. Sketch of active shock mount for interior noise reduction.

10.1.2. Measurements and simulations of noise from shallow-cavity flows

Low speed wind tunnel tests have been conducted to characterize wall pressure fluctuations generated by turbulent boundary layers over shallow cavities. A simplified incompressible flow model was designed to reproduce geometrical discontinuities present, for example on an aircraft fuselage, and responsible for interior noise generation. The experimental activity started as collaboration with CIRA (Italian Aerospace Research Center) under the ENABLE project of the fifth FP, and was aimed at the characterization of the pressure perturbations at the wall. Satisfactory scaling for both the OASPL and the frequency spectra by dimensionless parameters have been obtained and empirical correlations have been proposed to predict wall pressure properties in practical applications [43]. Mechanisms characterizing the pressure propagation have been also clarified in particular showing that close to the forward-step, the hydrodynamic contribution of the pressure fluctuations is accompanied by a relevant acoustic effect characterized by a convection velocity close to the speed of sound [44]. Research in this field is still in progress in collaboration with both CIRA and INSEAN (Italian Ship Model Basin) and is targeted towards the analysis of the correlation between the wall pressure statistics and the fluid dynamic structures present within the turbulent boundary layer overflowing the wall.

In addition, a non-standard, integral formulation for the identification of the acoustic spectrum of cavities has been developed [45]. For transportation vehicles, the importance of this problem is not only related to passenger comfort in cabin, but also to the dynamic response of elastic structures interacting with the pressure field arising around them (for instance, this problem concerns payloads inside launcher fairings). Using the fundamental solution of the Laplace operator, the formulation proposed identifies the spectrum through the solution of a standard eigenvalue problem. This approach avoids the difficulties that arise in calculating acoustic frequencies and modes of vibration when the Kirchhoff–Helmholtz boundary-integral operator is applied, because of the transcendental dependence on frequency of the Green function of the wave equation. [by R. Camussi, G. Guj, A. Di Marco, U. Iemma, M. Gennaretti. University ''Roma Tre'', camussi@uniroma3.it, Antonio Ragni, CIRA, Italy].

10.2. Measurements and predictions of community noise of a pusher-propeller general aviation aircraft

The stringent requirements imposed by the airworthiness rules in terms of acceptable noise levels of aircraft require nowadays a particular attention to this aspect. It is well known, in fact, that in some cases these very severe rules may reduce the operability of some airplanes, or, in extreme cases, may ground them.

The pusher-propeller configuration is more prone to these regulations than classical tractor-propeller aircraft, due to the added effect of the propeller-exhaust interaction, which generally increases up to critical values the noise levels transmitted to the community [46,47].

Based on these not negligible considerations, an intense research activity has been promoted between Piaggio Aero Industries and University of Naples ''Federico II'' for improving the knowledge of the problem and for investigating for possible applicable solutions to existing and future airplanes. This research activity has been directed toward both experimental and numerical activities, subdivided in different tasks.

In a first task the aeroacoustic field is predicted through different step by step CFD calculations to take into account all the perturbative effects (wing, flaps, fwd wing, aircraft body, exhaust, etc.) on the aerodynamics and thus on the acoustic field generated by the propeller [48–51].

The next task is the experimental one, where both ground and flight test on a prototype company aircraft are planned. So far some experimental tests have been performed on different exhaust shape and orientation configuration to define an optimal design capable to reduce the exhaust-propeller interference noise.

A final task is aimed to define a numerical tool that, on the basis of the single source noise characteristics, is capable to predict the aircraft Community Noise levels on the certification point [52–54], taking into account the different noise propagation and atmospheric effects. The tool is applicable for small and large aircraft, propeller and jet powered as well. The results of the research program have been also used for the initial steps of a new project and they show good reliability and possibility to effectively integrate the noise issues with the other requirements of the aircraft [by F.S. Marulo, U. Polimeno, F. Perna, University of Naples, A. Sollo, M. Aversano Piaggio Aero Industries SpA, Italy].

10.3. Analysis of the aeroacoustics of the VEGA launcher to estimate the payload vibroacoustic environment

The aeroacoustic environment created by the external aerodynamics around the VEGA launcher has been investigated through a research activity jointly carried out by CIRA, AVIO and the Department of Mechanical and Industrial Engineering of the University "Roma Tre".

The activity pursued in 2005 was based on the experimental measurements conducted during the last years and was mainly aimed at clarifying theoretical aspects correlated to the wall pressure statistical characterization and modelling. Specifically, the main issues faced are the following:

1. Extrapolation of the experimental data at full scale in both transonic and supersonic flow conditions (see [55] and [56]).
2. Characterization of the wall pressure perturbation propagation properties in the transonic flow conditions ([57], [58]).

As an example of the achieved results, the evolution of the wall pressure auto-spectra along the launcher model is reported in Fig. 48 for a transonic case [by G. Guj, R. Camussi, University "Roma Tre", A. Nicolì, B. Imperatore, CIRA, A. Pizzicaroli, Avio, Italy].

10.4. In-duct propagation in the high frequency range using a higher-order parabolic equation

Efficient methods are required to reduce fan noise radiated through aero-engine inlets. The methods have to predict in-duct propagation in the presence of liner absorption and flow effects. Numerical techniques such as BEM or FEM are restricted to the low and mid frequency range, due to the CPU time and memory requirements. Ray models, valid in the high frequency range, have limited application due to scattering effects and caustics associated with non-uniform flows. The Parabolic Equation method (PE) is an attractive alternative to predict duct propagation in the high frequency range. It uses an efficient marching algorithm to solve the forward propagating field. Boundary conditions are imposed at the duct entrance and on the duct walls, but no boundary is necessary at the duct exit. A higher-order parabolic equation (HOPE) derived from a high order Padé expansion has been developed to deal with the large aperture angle needed to compute

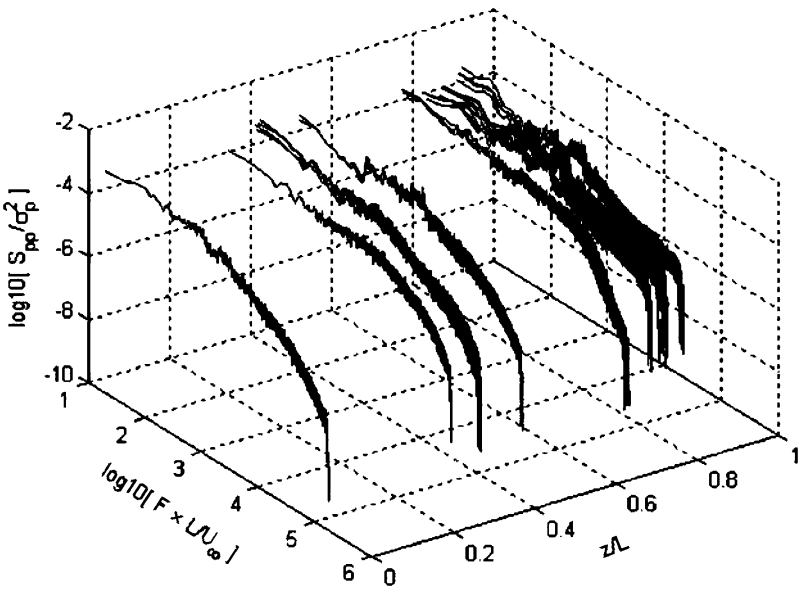

Fig. 48. Normalized auto-spectra evolution along the launcher model for $M = 0.98$ at $\alpha = 0°$. U_∞ is the mean velocity upstream the tested model in the wind tunnel conditions.

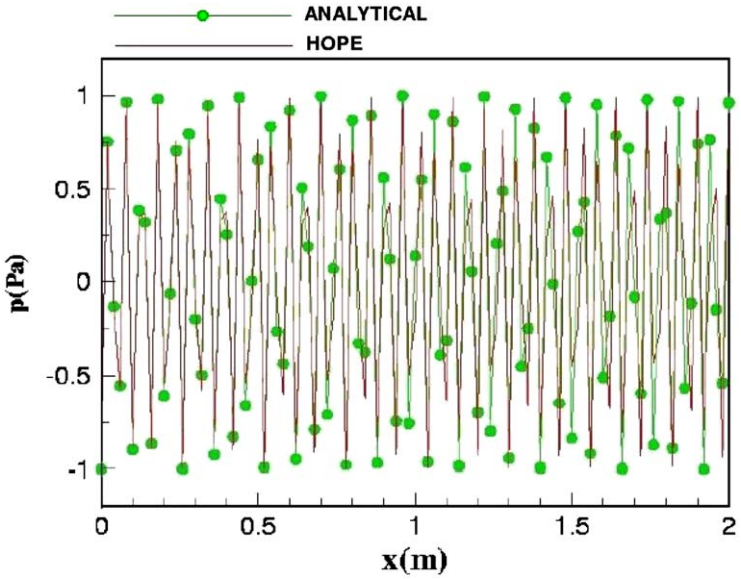

Fig. 49. Sound pressure propagation in a 2D duct. Comparison between the analytical and the numerical solutions: $f = 10\,\text{kHz}$, Mach $= -0.5$.

in-duct propagation, especially for frequencies close to cut-off [59]. Very good agreement has been obtained with the modal approach (Figs. 49 and 50) [by P. Malbéqui, ONERA, France, Patrice.malbequi@onera.fr].

10.5. Multidisciplinary aircraft optimisation for low noise

10.5.1. 'Silent' aircraft initiative

The "Silent Aircraft Initiative", a joint project between the University of Cambridge and MIT, funded by the Cambridge-MIT Institute (CMI), has completed its first conceptual aircraft design, Fig. 51. Based on a highly integrated aircraft with embedded engines, it provides good shielding of forward propagating engine noise and space for extensive acoustic liners. The engine bypass ratio is about twice that of current technology and is chosen to reduce the jet noise. A variable area exit nozzle reduces the bypass ratio in cruise to give good fuel consumption. Work is in progress on further iterations in the aircraft configuration and operations, together with improved fidelity noise estimates. The target is for a conceptual design of an aircraft whose noise will be imperceptible outside the airfield perimeter in an urban environment. [by A. Dowling, University of Cambridge, UK apd1@eng.cam.ac.uk].

10.5.2. Design optimization including noise issues

A research activity dealing with the inclusion of aeroacoustic issues in a multidisciplinary design optimization (MDO) environment has been recently started. The noise reduction imposed in the near future by the recently approved regulations will be hardly fulfilled by simply improving the current aircraft configurations. The need of highly innovative concept is a must and represents, nowadays, a design challenge of the primary importance. Indeed, when dealing with innovative configurations, the designer can't rely solely on the past experience, and must be assisted by integrated, multidisciplinary, prime-principle-based tools. The development of the code MAGIC+ (Multidisciplinary Aircraft desiGn of Innovative Configurations) is currently focused on that goal. The noise is taken into account within the MDO framework in the form of an additional operational cost. This non-conventional approach is justified by the increasing amount of the "noise tax" due by airlines to operate in all the major airports, which is making "noisy" fleets much more expensive that before. Preliminary results, obtained with a very simple noise model and with a limited number of degrees of freedom (only the wing system is optimized, with payload, fuselage and propulsion prescribed)

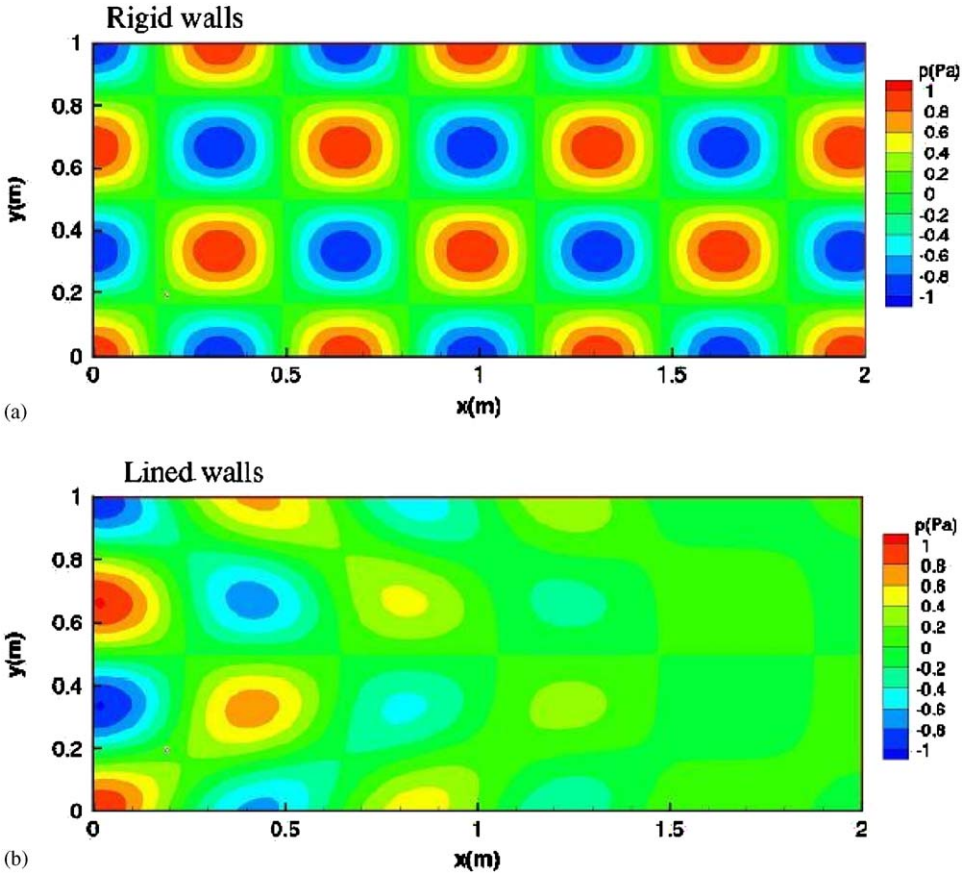

Fig. 50. Sound pressure field in a 2D duct with rigid (a) and lined walls (b). $f = 1$ kHz, Mach $= 0.5$.

Fig. 51. 'Silent' Aircraft Initiative.

show that the life-cycle-cost can be reduced with the inclusion of the "cost of the noise" within the preliminary phase of the design. The implementation of more accurate aeroacoustic models is in course of development, as well as the introduction of additional noise-related variables in the MDO (e.g., engines by-pass ratio, high-lift devices operative conditions, etc.) to verify and validate the observed trend [60] [by U. Iemma, M. Diez, University "Roma Tre", Italy, u.iemma@uniroma3.it].

References

[1] A. McAlpine, M.J. Fisher, On the prediction of "buzz-saw" noise in aero-engine inlet ducts, *Journal of Sound and Vibration* 248 (1) (2001) 123–149.

[2] A. McAlpine, M.J. Fisher, On the prediction of "buzz-saw" noise in acoustically lined aero-engine inlet ducts, *Journal of Sound and Vibration* 265 (1) (2003) 175–200.

[3] A. McAlpine, M.J. Fisher, B.J. Tester, Buzz-saw noise: a comparison of measurement with prediction, *Journal of Sound and Vibration* 290 (2006) 1202–1233.

[4] G. Gabard, R.J. Astley, Theoretical model for sound radiation from annular jet pipes: far- and near-field solutions, *Journal of Fluid Mechanics* 549 (2006) 315–341.

[5] D. Sutliff, M. Nallasamy, L. Heidelberg, D. Elliott, Baseline acoustic levels of the NASA active noise control fan rig, NASA Technical memorandum 107214, 1996.

[6] S. Redonnet, E. Manoha, O. Kenning, Numerical Simulation of the Downstream Fan Noise of 3D Coaxial Engines, in: *AIAA 2005-2816, Eleventh AIAA/CEAS Aeroacoustics Conference*, Monterey, USA, 2005.

[7] C. Polacsek, S. Burguburu, S. Redonnet, M. Terracol, Numerical Simulations of Fan Interaction Noise Using a Hybrid Approach, *AIAA 2005-2814, Eleventh AIAA/CEAS Aeroacoustics Conference*, Monterey, USA, 2005.

[8] Jordan, Coiffet, Delville, Gervais, Ricaud, Coherent structures in subsonic jets: a quasi-irrotational source mechanism? *International Journal of Aeroacoustics* 5(1) (2006).

[9] T. Jordan, D. Coiffet, H. Glauser, Low-dimensional signatures of the sound production mechanisms in subsonic jets: Towards identification and control, Invited paper, *Thirty-fifth AIAA Fluid Dynamics Conference*, Toronto, ON, Canada, 2005.

[10] S. Lévy, Prediction of turbofan rotor or stator broadband noise radiation, *Inter-noise 2005*, Rio de Janeiro, Brazil, 7–10 August 2005.

[11] R. Arina, Numerical Method for the Convected Lighthill's Equation, in: *AIAA 2005-2928, Eleventh AIAA/CEAS Aeroacoustics Conference*, 23–25 May 2005, Monterey, CA, USA.

[12] S.W. Rienstra and N. Peake, Modal scattering at an impedance transition in a lined flow duct, in: *AIAA Paper No. 2005-2852, Eleventh AIAA/CEAS Aeroacoustics Conference*, 23–25 May 2005, Monterey CA, USA.

[13] S.W. Rienstra, B.T. Tester, An Analytic Green's Function for a Lined Circular Duct Containing Uniform Mean Flow, in: *AIAA 2005-3020, Eleventh AIAA/CEAS Aeroacoustics Conference*, Monterey, CA, 23–25 May 2005.

[14] G.G. Vilenski, S.W. Rienstra, Acoustic Modes in a Ducted Shear Flow, in: *AIAA 2005-3024, Eleventh AIAA/CEAS Aeroacoustics Conference*, Monterey, CA, 23–25 May 2005.

[15] P.B. Murray, P. Ferrante, A. Scofano, Manufacturing process and boundary layer influences on perforate liner impedance, in: *AIAA 2005-2849*, 2005.

[16] L.M.B.C. Campos, J.M.G.S. Oliveira, On the acoustic modes in a cylindrical duct with an arbitrary impedance distribution, *Journal Acoustical Society America* 116, 3336–3347.

[17] L.M.B.C. Campos, J.M.G.S. Oliveira, On the optimisation of acoustic liners in annular nozzles, *Journal of Sound and Vibration* 275, 557–576.

[18] M. Lummer, J.D. Delfs, Th. Lauke, Simulation of sound generation by vortices passing the trailing edge of airfoils, in: *AIAA 2002-2578, Eighth AIAA/CEAS Aeroacoustic Conference*, 17–19 June 2002, Breckenridge, CO.

[19] R. Ewert, CAA Slat noise studies applying sound sources based on solenoidal digital filters, in: *AIAA Paper 2005-2862*, 2005.

[20] O. Marsden, C. Bogey, C. Bailly, Noise radiated by a high-Reynolds-number 3D airfoil, in: *Eleventh AIAA/CEAS Aeroacoustics Conference*, 23–25 May, Monterey, USA, AIAA Paper 2005-2817. See also AIAA Paper 2006-2503.

[21] R. Ewert, W. Schröder, Acoustic perturbation equations based on flow decomposition via source filtering, *Journal of Comparative Physics* 188 (2003) 365–398.

[22] T. Ph Bui, M. Meinke, W. Schröder, F. Flemming, A. Sadiki, J. Janicka, A hybrid method for combustion noise based on LES and APE, in: *AIAA Paper 2005-3014*, 2005.

[23] E. Gröschel, M. Meinke, W. Schröder, Noise prediction for a turbulent jet using an LES/CAA method, in: *AIAA Paper 2005-3039*, 2005.

[24] J. Yin, B.V.D. Wall, S. Oerlemans, Representative test results from HeliNoVi aeroacoustic Main Rotor/Tail Rotor/Fuselage test in DNW, in: *Thirty-first European Rotorcraft Forum, 2005, paper 42*, Florence, Italy.

[25] H.-J. Langer, O. Dieterich, S. Oerlemans, O. Schneider, B.V.D. Wall, J. Yin, The EU HeliNOVI Project-wind tunnel investigations for noise and vibration reduction, in: *Thirty-first European Rotorcraft Forum 2005, Paper 32*, Florence, Italy.

[26] M. Gennaretti, G. Bernardini, A novel potential-flow boundary integral formulation for helicopter rotors in BVI conditions, in: *AIAA Paper 2005-2924, Eleventh AIAA/CEAS Aeroacoustics Conference*, Monterey, CA, May 2005.

[27] S. Oerlemans, B. Méndez López, Acoustic array measurements on a full scale wind turbine, in: *AIAA Paper 2005-2963, Eleventh AIAA/CEAS Aeroacoustics Conference*, 23–25 May 2005, Monterey, CA.

[28] B. Müller: Towards high order numerical simulation of aeolian tones, in: *Proceedings in Applied Mathematics and Mechanics*, 2005 (submitted).

[29] B. Müller, High order numerical simulation of aeolian tones. *Computers & Fluids* 2005 (submitted).

[30] W. De Roeck, G. Rubio, Y. Reymen, J. Meyers, M. Baelmans, W. Desmet, Towards accurate flow and acoustic prediction techniques for cavity flow noise applications, in: *AIAA-paper 2005-2978, Eleventh AIAA/CEAS Aeroacoustics Conference*, Monterey, CA, USA, 2005.

[31] G. Rubio, W. De Roeck, M. Baelmans, W. Desmet, Numerical identification of flow-induced oscillation modes in rectangular cavities, in: *Third International Conference on Advanced Computational Methods in Engineering ACOMEN 2005*, Gent, Belgium, 2005.

[32] G. Rubio, W. De Roeck,, Y. Reymen, J. Meyers, M. Baelmans, W. Desmet, A hybrid flow-acoustic prediction technique with application to 2D cavity flow noise, in: *Twelth International Congress on Sound and Vibration ICSV12*, Lisbon, Portugal, 2005.
[33] P. Batten, U.C. Goldberg, S.R. Chakravarthy, Interfacing statistical turbulence closures with large eddy simulation, *AIAA Journal* 42(3) (2004).
[34] P. Batten, E. Ribaldone, M. Casella, S.R. Chakravarthy, Towards a generalized non-linear acoustics solver, in: *AIAA 2004-3001, Tenth AIAA/CEAS Aeroacoustics Conference*, Manchester, UK, 2004.
[35] E., Sarradj, C. Schulze, A. Zeibig, Identification of noise source mechanisms using orthogonal beamforming, in: *Proceedings of Noise and Vibration: Emerging Methods' Conference*, St. Raphael, 2005.
[36] P. Di Francescantonio, D. Casalino, Green's function discretization scheme for sound propagation in nonuniform flows, *AIAA Journal* 37 (10) (1999) 1161–1172.
[37] P. Di Francescantonio, D. Casalino, L. De Mercato, Aeroacoustic design of aero-engine intake liners, in: *AIAA 2005-2942, Eleventh AIAA-CEAS Aeroacoustics Conference*, 2005.
[38] R. Arina, M. Falossi, Domain decomposition technique for aeroacoustic simulations, *Applied Numerical Mathematics* 49 (3&4) (2004) 263–275.
[39] R. Arina, Numerical Method for the Convected Lighthill's Equation, in: *AIAA 2005-2928, Eleventh AIAA/CEAS Aeroacoustics Conference*, 23–25 May 2005, Monterey, CA, USA.
[40] R. Arina, M. Falossi, Multi-block curvilinear grid scheme for aeroacoustic flow predictions, in: *EUROMECH-449 Computational Aeroacoustics: From Acoustic Sources Modeling to Far-Field Radiated Noise Prediction*, 9–12 December 2003, Chamonix, France.
[41] L.M.B.C. Campos, P.G.T.A. Serrão, On the acoustics of unbounded and ducted vortex flows, *SIAM Journal of Applied Mathematics* 65, 1353–1368.
[42] S. Tewes, R. Maier, A. Peiffer, Active trim panel attachments for control of sound transmission through aircraft structures, in: *Ninth CEAS-ASC Workshop. Active Control of Aircraft Noise: Concept to Reality*, KTH Stockholm, Sweden, 2005.
[43] R. Camussi, G. Guj, A. Ragni, Wall pressure fluctuations induced by turbulent boundary layers over surface discontinuities, *Journal of Sound and Vibration*, in press (also *Proceedings of the Fifteenth Australasian Fluid Mechanics Conference*, The University of Sydney, Sydney, Australia, 13–17 December 2004).
[44] R. Camussi, G. Guj, A. Di Marco, A. Ragni, Propagation of wall pressure perturbations in a large aspect-ratio shallow cavity, Experiments in Fluids, in press (also *Proceedings of the ERCOFTAC International Symposium on Engineering Turbulence Modelling and Measurements ETMM6*, Sardinia, Italy, 23–25 May 2005).
[45] U. Iemma, M. Gennaretti, A boundary-field integral equation for analysis of cavity acoustic spectrum, *Journal of Fluids and Structures* 45 (2006) 261–272.
[46] G. Neuwerth, Th. Lölgen, R. Staunfenbiel, Increased noise emission of propellers and propfans due to pusher installation, in: *Proceedings of ICAS 1990*, pp. 127–138.
[47] D.S. Weir, M. Marsan, C. Lyon, Acoustical analysis capability for Pusher Propeller installations, in: *Proceedings of Twenty-Eighth Aerospace Sciences Meeting*, 1990.
[48] P.T. Soderman, W. Clifton Horne, Acoustic and aerodynamic study of a Pusher-Propeller aircraft model, NASA TP-3040, 1990.
[49] A. Massardo, F. Dotta, Analisi sperimentale del rumore generato da eliche in configurazione spingente, Atti del 51° Congresso ATI, Udine, Italy, 1996, pp. 1385–1398 (in Italian).
[50] A. Sollo, M. Aversano, A. Di Mascio, S. Ianniello, F. Salvatore, M. Gennaretti, Evaluation of noise excess for pushing propeller aircraft by CFD aeroacoustic calculation, in: *Proceedings of the Tenth AIAA/CEAS Aeroacoustic Conference 2004*, Manchester Town Hall, 2004.
[51] C. Mauk, S. Farokhi, The effect of unsteady blade loading on the aeroacoustics of a pusher propeller, in: *Proceedings of the AIAA/SAE/ASME/ASEE 29th Joint Propulsion Conference and Exhibit*, 1993.
[52] JAR-36 SUBPART C—Propeller Driven Airplanes Not Exceeding 9000 Kg. Application for Type Certification or Certification of Derived Version accepted on or after 1 July 1996. Issue 23 May 1997.
[53] Part 36—Noise Standards: Aircraft type and airworthiness certification, FAA, DOT, revised as of January 2003.
[54] ICAO—International Standards and Recommended Practices—Environmental Protection Annex 16 to the Convention on International Civil Aviation—Aircraft Noise. Vol. I, second ed., 1993.
[55] G. Guj, B. Imperatore, A. Pizzicaroli, R. Camussi, A. Ragni, E. Giulietti, A. Nicolì, A. Di Marco, Experimental activity for modelling the external aeroacoustic of the VEGA, in: *Proceedings of XVIII AIDAA Conference*, Volterra (Pi, Italy), 9/2005.
[56] B. Imperatore, G. Guj, A. Ragni, A. Pizzicaroli, Aeroacoustic of the VEGA launcher wind tunnel tests and full scale extrapolations, in: *AIAA paper 2005-2913, Eleventh AIAA/CEAS Aeroacoustics Conference*, Monterey, CA, USA, 5/2005.
[57] G. Guj, R. Camussi, A. Di Marco, B. Imperatore, Pressure fluctuations in the transonic boundary layer of a VEGA launcher model, in: *AIAA paper 2005-2856, Eleventh AIAA/CEAS Aeroacoustics Conference*, Monterey, CA, USA, 5/2005.
[58] R. Camussi, G. Guj, B. Imperatore, A. Pizzicaroli, D. Perigo, Wall pressure fluctuations induced by transonic boundary layers on a launcher model, *Journal Aerospace Science and Technology* (2005, submitted).
[59] P. Malbéqui, Duct propagation using a higher order parabolic equation, in: *Proceedings of Eleventh International Congress on Sound and Vibrations*, St. Petersburg, Russia, 5–8 July 2004.
[60] U. Iemma, M. Diez, L. Morino, Community noise impact on the conceptual design of innovative aircraft configurations, in: *AIAA 2005-2982, Eleventh AIAA/CEAS Aeroacoustics Conference*, Monterey, CA, 23–25 May 2005.